*Physics and the Cosmos*
https://www.sciltp.com/journals/pac

*Review*

# Clues of New Physics from Gamma-Ray Burst GRB 221009A

Giorgio Galanti [1,*], Marco Roncadelli [2,3,*] and Fabrizio Tavecchio [3,*]

[1] INAF, Istituto di Astrofisica Spaziale e Fisica Cosmica di Milano, Via Alfonso Corti 12, I-20133 Milano, Italy
[2] INFN, Sezione di Pavia, Via Agostino Bassi 6, I-27100 Pavia, Italy
[3] INAF, Osservatorio Astronomico di Brera, Via Emilio Bianchi 46, I-23807 Merate, Italy
[*] Correspondence: gam.galanti@gmail.com (G.G.); marcoroncadelli@gmail.com (M.R.); fabrizio.tavecchio@inaf.it (F.T.)

**How To Cite**: Galanti, G.; Roncadelli, M.; Tavecchio, F. Clues of New Physics from Gamma-Ray Burst GRB 221009A. *Physics and the Cosmos* **2025**, *1*(1), 2.

Received: 10 October 2025
Revised: 11 November 2025
Accepted: 19 November 2025
Published: 5 December 2025

**Abstract:** The discovery of the gamma-ray burst GRB 221009A is one of the most important observations in contemporary astrophysics. Not only is GRB 221009A an exceptionally bright and rare event estimated to occur once in 5000 years, but it is the gamma-ray burst observed at the highest energy so far. LHAASO detected GRB 221009A up to $\sim$15 TeV and Carpet even up to $\sim$300 TeV. Since within the standard propagation model photons are not expected to be observed above 10 TeV at the distance of GRB 221009A for any reasonable emission model—due to the interaction with background photons—such a detection also represents a milestone in the search for new physics. In the present review we show that *two effects of new physics* are indeed necessary to explain GRB 221009A. (1) Axion-like particles (ALPs) account for the LHAASO observations but are ineffective at Carpet energies. (2) Lorentz invariance violation (LIV) is instead complementary, being ineffective for LHAASO but explaining the Carpet detection. Therefore, GRB 221009A suggests a new physical ALP + LIV scenario in which *photon-ALP oscillations take place in a LIV background*.

**Keywords:** particle physics; astroparticle physics; axion-like particles; quantum gravity; Lorentz invariance violation; gamma-ray burst: GRB 221009A

## 1. Introduction

A revolutionary discovery has been made on 9 October 2022 when the exceptionally bright gamma-ray burst GRB 221009A at redshift $z = 0.151$ [1–3] was observed by the Swift satellite mission [4] and by the Fermi Gamma-ray Burst Monitor (Fermi-GBM) aboard the *Fermi* satellite [5,6]. This is the brightest gamma-ray burst (GRB) ever observed, so bright to ionize the upper ionosphere and to deserve the name *brightest of all times* (BOAT) [7]. Besides, GRB 221009A is unique also in another respect, since its photon emission has reached the terrific energy of $\sim$300 TeV.

The aim of this paper is to review the arguments whereby the observation of photons from GRB 221009A of energy $\mathcal{E} > 10$ TeV challenges conventional physics and provides two distinct clues of new physics in the form of specific *axion-like particles* (ALPs) [8] and *Lorentz invariance violation* (LIV) at a scale not too far from the Planck mass [9], which is the first observational evidence of a long sought low-energy manifestation of quantum gravity.

## 2. General Features of GRBs

GRBs are extremely energetic explosions which give rise to collimated jets of plasma where particles are accelerated at ultra-relativistic energies. They are characterized by two phases: an initial *prompt* and a subsequent *afterglow*. Moreover, GRBs fall into two classes. *Short* GRBs with the prompt emission lasting less than 2 s originate from the merging of two neutron stars (or a neutron star with a black hole), whereas *long* GRBs with the prompt emission exceeding 2 s arise from ultra-relativistic jets launched from the collapsing cores of dying massive stars. GRB 221009A has been classified as a long one.

The prompt emission arises from the dynamical activity of the implosion, is highly variable and reaches its maximum typically in the keV–MeV energy range. Its duration lasts from milliseconds to minutes. Thereafter, the afterglow emission takes over—also rapidly varying—which is due to the shock waves of the GRB expanding into the external medium and can last up to months. The highest frequency photons are generated at the beginning of the afterglow, and as time goes by photons of progressively lower and lower frequencies are emitted, spanning the whole electromagnetic spectrum from the gamma-ray band down to the radio band. While it is generally believed that the prompt emission is explained as synchrotron radiation by electrons accelerated in the GRB magnetic field, the *spectral energy distribution* (SED) of the afterglow is not so simple (more about this, in Section 9). We emphasize that this is the conventional view based on the relativistic fireball model [10–12]. Nevertheless, alternative models have been proposed, which will be shortly reviewed in Section 9.

## 3. Observation of Very-High-Energy Photons from GRB 221009A

Conventionally, *very-high-energy* (VHE) photons are in the energy range $100\,\mathrm{GeV} < \mathcal{E} < 100\,\mathrm{TeV}$. Before addressing the physical implications of GRB 221009A it seems quite instructive to recall the observations of its VHE photons in a quantitative fashion.

More than 5000 photons have been recorded by the Water Cherenkov Detector Array (WCDA) of the LHAASO collaboration at $\mathcal{E} > 500\,\mathrm{GeV}$ during the first 2000 s after the Fermi-GBM trigger time, henceforth referred to as the *trigger*. In addition, 142 photon-like events have been registered by the KM2A detector—also of the LHAASO collaboration—in the energy range $3\,\mathrm{TeV} \leq \mathcal{E} \leq 20\,\mathrm{TeV}$ over the time lapse $230\,\mathrm{s} \leq t \leq 900\,\mathrm{s}$ after the trigger, 8 of which with $\mathcal{E} > 10\,\mathrm{TeV}$. The maximal photon energy estimated by the LHAASO collaboration depends on the assumed spectral function used to fit the data, resulting in $17.8^{+7.4}_{-5.1}\,\mathrm{TeV}$ for a log-parabola (LP) and $12.5^{+3.2}_{-2.4}\,\mathrm{TeV}$ for a power-law with an exponential cutoff (PLEC). Note that in the latter case the highest energy point has an unphysical turn up, and so the former case seems preferable: this explains why we have quoted $\sim 15\,\mathrm{TeV}$. Specifically, the LHAASO collaboration considers two time intervals: $230\,\mathrm{s} < t < 300\,\mathrm{s}$ and $300\,\mathrm{s} < t < 900\,\mathrm{s}$. Their fit with a LP gives $\chi^2/\mathrm{ndf} = 14.1/9 \simeq 1.57$ and $\chi^2/\mathrm{ndf} = 37.3/10 \simeq 3.73$ for the considered time intervals, where ndf is the number of degrees of freedom. Instead, the fitting with a PLEC similarly yields $\chi^2/\mathrm{ndf} = 10.1/9 \simeq 1.12$ and $\chi^2/\mathrm{ndf} = 18.3/10 \simeq 1.83$. Because the fit with a PLEC has a smaller reduced $\chi^2$ this value is preferred [13]. Of course, fits with other spectral functions yield different maximal photon energies. So, what is the best fitting spectral function? In addition, what is the meaning of a statistical analysis over only 10 degrees of freedom? The same *emitted* power-law spectrum ultimately fits the photons observed by both the WCDA and KM2A detectors. These results have first been reported in an astronomical telegram just after the detection [14] and next in two different papers, both published in 2023 [13,15].

Preliminary evidence for a single photon of energy $\mathcal{E} \simeq 251\,\mathrm{TeV}$ at $t = 4536\,\mathrm{s}$ after the trigger—coincident both spatially and temporarily with GRB 221009A—has been reported by the Carpet collaboration in an astronomical telegram soon after the detection [16], but the result of the full data analysis has been published only in May 2025 [17]. The reason for this delay is due to the configuration of the Carpet apparatus. Besides photon detectors, it consists of an inner small-area muon (ISAM) detector and four outer large-area muon (OLAM) detectors, all of which were operative at the time of the GRB 221009A observation. However, the first result reported in the astronomical telegram [16] was based *only* on the data collected over $4536\,\mathrm{s}$ by the ISAM detector, and it took a very long time to analyze the *whole* data set collected over *one day* [17]. Muon detectors play a key-role in discriminating between a primary photon emitted by GRB 221009A and a secondary photon originating from proton-proton collisions in a ultra-high-energy cosmic ray shower, since in the latter case also pions are produced. Neutral pions decay into two photons while charged pions decay into neutrinos and muons. In either case, these decay products can be recorded on Earth. So, the lack of muon detection by the Carpet collaboration is a proof that their observed photon indeed comes from GRB 221009A. Quantitatively, the probability that the observed photon is a misidentified hadron is as small as $3 \cdot 10^{-4}$. In addition, the same *emitted* power-law spectrum which ultimately fits the photons observed by both the WCDA and the KM2A detectors of the LHAASO collaboration is in order-of-magnitude agreement with the Carpet event when extrapolated to much higher energies. The updated result is a single photon-like event of energy $\mathcal{E} = 300^{+43}_{-38}\,\mathrm{TeV}$ coincident—with chance probability of about $9 \cdot 10^{-3}$—with GRB 221009A in its arrival direction and time. Finally, according to the Carpet collaboration the reason why their photon event has not been observed by the LHAASO and the HAWC collaborations is that it was close to the limit of the field of view of the LHAASO detectors, whereas the line of sight of the HAWC detector to GRB 221009A was below the horizon. Thus, the new Carpet result looks robust.

## 4. First Challenge to Conventional Physics

The observation of photons with energy $\mathcal{E} > 10\,\mathrm{TeV}$ is strongly in tension with conventional physics. The reason is as follows. The infrared/optical/ultraviolet light emitted by all galaxies during the whole cosmic evolution forms the *extragalactic background light* (EBL) [18]. When a VHE photon from GRB 221009A scatters off an EBL photon through the $\gamma\gamma \to e^+e^-$ process [19,20] there is a chance to produce an $e^+e^-$ pair, which causes the VHE photon to be absorbed. Within conventional physics this effect is quantified by the optical depth $\tau_{\mathrm{CP}}(\mathcal{E}, z)$, which is an *increasing* function of both energy $\mathcal{E}$ and redshift $z$ [21–25]. In order to evaluate $\tau_{\mathrm{CP}}(\mathcal{E}, z)$ a model of the EBL is needed, which must be derived from observations. In [8] the Saldana-Lopez et al. EBL model [26] is adopted because of four different reasons: (1) it is the most recent one, (2) it is based on the deepest galaxy dataset ever obtained, (3) it is derived by a satellite borne detector, which minimizes the foreground effects (like zodiacal light), and (4) it has been used by the LHAASO collaboration.

We work within the standard spatially flat cosmological model with $\Omega_{\mathrm{M}} = 0.3$, $\Omega_{\Lambda} = 0.7$ and $H_0 = 70\,\mathrm{km}\cdot\mathrm{s}^{-1}\cdot\mathrm{Mpc}^{-1}$. Once the optical depth is known [23], the photon survival probability is given by

$$P_{\mathrm{CP}}(\mathcal{E}, z; \gamma \to \gamma) = e^{-\,\tau_{\mathrm{CP}}(\mathcal{E}, z)}\,. \tag{1}$$

Moreover, the observed flux $\mathcal{F}_{\mathrm{obs}}(\mathcal{E}, z)$ is related to the emitted one $\mathcal{F}_{\mathrm{em}}(\mathcal{E}(1+z))$ as

$$\mathcal{F}_{\mathrm{obs}}(\mathcal{E}, z) = P_{\mathrm{CP}}(\mathcal{E}, z; \gamma \to \gamma)\, \mathcal{F}_{\mathrm{em}}\big(\mathcal{E}(1+z)\big) = e^{-\,\tau_{\mathrm{CP}}(\mathcal{E}, z)}\, \mathcal{F}_{\mathrm{em}}\big(\mathcal{E}(1+z)\big)\,. \tag{2}$$

An explicit calculation shows that for $z = 0.151$ photons of $\mathcal{E} > 10\,\mathrm{TeV}$ tend to be fully absorbed by the EBL for any reasonable GRB emission model [8]. Thus, the bottom line is that photons of $\mathcal{E} > 10\,\mathrm{TeV}$ from GRB 221009A should *not* be observed according to conventional physics.

## 5. Motivation for Axion-Like Particles (ALPs)

Given the above conclusion, the fundamental question arises of how to reduce the cosmic opacity brought about by the EBL. In order to understand—and appreciate—how this comes about it seems appropriate to start from a general consideration.

Nowadays, the Standard Model of particle physics is regarded as the low-energy manifestation of a more fundamental theory which unifies the four basic interactions at the quantum level. Every specific approach to accomplish this task is characterized by a set of new particles, along with their specific mass spectrum and their interactions with the standard world. Even though it is presently impossible to tell which proposal—out of so many ones—has a good chance to achieve the goal, it is nevertheless remarkable that several attempts along very different directions such as four-dimensional supersymmetric models [27–31], multidimensional Kaluza-Klein theories [32,33] and especially M theory—which encompasses superstring and superbrane theories—generically predict the existence of ALPs (for a more detailed motivation see [34, 35], for reviews see [36–38] and for a very incomplete list of references, see [39–57]). They are very light pseudo-scalar particles quite similar to the axion [58–60], but they differ in two respects: (1) ALPs couple only to two photons (other couplings are possible but not compelling and are here discarded), and (2) the ALP mass $m_a$ and the two-photon coupling $g_{a\gamma\gamma}$ are fully *unrelated*, hence treated as free parameters. Thus, the only new term to be added in the Standard Model Lagrangian is

$$\mathcal{L}_{\mathrm{ALP}} = \frac{1}{2}\,\partial^{\mu} a\, \partial_{\mu} a - \frac{1}{2}\, m_a^2\, a^2 + g_{a\gamma\gamma}\, \mathbf{E}\cdot\mathbf{B}\, a\,, \tag{3}$$

where $a$ denotes the ALP field. Throughout this review we work in the presence of an external magnetic field $\mathbf{B}$, and so $\mathbf{E}$ stands for the electric field of a propagating photon. Therefore, owing to the last term in Equation (3) an off-diagonal element in the mass matrix for the photon-ALP system shows up. Correspondingly, the interaction eigenstates differ from the mass eigenstates and a photon-ALP mixing occurs. Moreover, the photon-ALP mixing gives rise to photon-ALP *oscillations*—as first pointed out in 1986 by Maiani, Petronzio and Zavattini [61]—which are analogous to neutrino oscillations but the magnetic field is needed to compensate for the spin mismatch. In particular, ALPs produce astrophysical effects both on the observed source spectra (see e.g., [62–71]) and on the observed photon polarization (see e.g., [72–81]). As long as we are concerned with GRB 221009A the redshift-dependence of the various quantities will be dropped. As first noted in 1988 by Raffelt and Stodolsky [82], when $\mathcal{E} \gg m_a$—which is certainly the present case—the photon-ALP beam propagation equation along the $y$ axis becomes

$$\left(i\,\frac{d}{dy}+\mathcal{E}+\mathcal{M}(\mathcal{E},y)\right)\left(\begin{array}{c}A_x(y)\\A_z(y)\\a(y)\end{array}\right)=0 \tag{4}$$

with $A_x(y)$, $A_z(y)$ denoting the two photon linear polarization amplitudes along the $x$ and $z$ axes, respectively, and $a(y)$ stands for the ALP amplitude. $\mathcal{M}(\mathcal{E},y)$ is the photon-ALP mixing matrix which fails to be self-adjoint when photon absorption by the EBL is taken into account. Observe that we are dealing with a Schrödinger-like equation with $t$ replaced with $y$, which entails that the beam propagation is formally described as a *non-relativistic three-level decaying quantum system*. This fact greatly simplifies the present treatment. Considering photons as unpolarized for the sake of simplicity, we use the polarization density matrix

$$\rho(y)=\left(\begin{array}{c}A_x(y)\\A_y(y)\\a(y)\end{array}\right)\otimes\left(\begin{array}{ccc}A_x(y)&A_y(y)&a(y)\end{array}\right)^{*}\,, \tag{5}$$

which obeys the Liouville-Von Neumann equation

$$i\frac{d\rho(y)}{dy}=\rho(y)\,\mathcal{M}^{\dagger}(\mathcal{E},y)-\mathcal{M}(\mathcal{E},y)\,\rho(y) \tag{6}$$

associated with Equation (4). Its solution is

$$\rho(y)=\mathcal{U}(\mathcal{E};y,y_0)\,\rho(y_0)\,\mathcal{U}^{\dagger}(\mathcal{E};y,y_0) \tag{7}$$

in terms of the transfer matrix $\mathcal{U}(\mathcal{E};y,y_0)$, namely the solution of Equation (4) with initial condition $\mathcal{U}(\mathcal{E};y_0,y_0)=1$. Then, the probability that a photon-ALP beam initially in the state $\rho_0$ at position $y_0$ will be found in the state $\rho$ at the final position $y$ is

$$P_{\rho_0\to\rho}(\mathcal{E};y)=\mathrm{Tr}\left(\rho\,\mathcal{U}(\mathcal{E};y,y_0)\,\rho_0\,\mathcal{U}^{\dagger}(\mathcal{E};y,y_0)\right)\,. \tag{8}$$

We are now in a position to understand why photon-ALP oscillations can allow for the observability of photons otherwise absorbed by the EBL, as first noted in 2007 by De Angelis, Roncadelli and Mansutti [62]. As a matter of fact, in the presence of a magnetic field they provide the photons with a split personality. Indeed, when they propagate as true photons they are absorbed but when they behave as ALPs they do *not*, since ALPs do not effectively couple either to *single* photons or to matter, as explicitly shown in [83]. Hence we have $\tau_{\rm ALP}(\mathcal{E})<\tau_{\rm CP}(\mathcal{E})$. Now, the crux of the argument is that Equation (1) gets replaced with

$$P_{\rm ALP}(\mathcal{E};\gamma\to\gamma)=e^{-\tau_{\rm ALP}(\mathcal{E})}\,, \tag{9}$$

so that even a *small* reduction of $\tau_{\rm ALP}(\mathcal{E})$ with respect to $\tau_{\rm CP}(\mathcal{E})$ leads to a *very large* increase of $P_{\rm ALP}(\mathcal{E};\gamma\to\gamma)$ as compared with $P_{\rm CP}(\mathcal{E};\gamma\to\gamma)$.

## 6. Photon-ALP Interconversions

Basically we follow the approach reported in [8]. It can schematically be summarized as follows.

*ALP parameters* —As benchmark values we take $m_a\simeq10^{-10}\,$eV, in line with previous works [8,66,71], and the two-photon coupling as $g_{a\gamma\gamma}\simeq4\cdot10^{-12}\,\mathrm{GeV}^{-1}$ in order to meet the strongest upper bound coming from the magnetized white dwarfs (MWD), which reads $g_{a\gamma\gamma}\lesssim5.4\cdot10^{-12}\,\mathrm{GeV}^{-1}$ at the $2\sigma$ level for $m_a\lesssim3\cdot10^{-7}\,$eV, even though it may turn out to be too strong owing to foreground effects [84]. However, the allowed parameter space is considerably wider, to wit $10^{-11}\,\mathrm{eV}\lesssim m_a\lesssim10^{-7}\,\mathrm{eV}$ and $3\cdot10^{-12}\,\mathrm{GeV}^{-1}\lesssim g_{a\gamma\gamma}\lesssim5\cdot10^{-12}\,\mathrm{GeV}^{-1}$ [8].

*Photon-ALP oscillations in GRB 221009A*—Recalling the previous discussion, the highest energy photons should be emitted at the onset of the afterglow, in the downstream region of the forward shock. In the shocked region photons travel a distance of order $R'/\Gamma$ in the co-moving frame, where $R'$ denotes the distance from the central engine whereas $\Gamma$ is the bulk Lorentz factor. Realistic values are $R'\simeq2\cdot10^{17}\,$cm, $\Gamma\simeq45$, co-moving electron density $n'_e\simeq450\,\mathrm{cm}^{-3}$ and co-moving magnetic field strength $B'\simeq2\,$G. In terms of these quantities the corresponding transfer matrix is computed, which turns out to be $\mathcal{U}_1(\mathcal{E};y_2,y_1)\simeq1$, where $y_2$ and $y_1$ are the position of the border of GRB 221009A and of the production region, respectively. Manifestly, in such a situation no appreciable photon-ALP oscillation takes place.

*Photon-ALP oscillations in the host galaxy*—GRB 221009A is located close to the nuclear region of a disk galaxy observed nearly edge-on [85,86], which is likely to be a normal spiral. As a consequence, the photon-ALP beam propagates mainly inside the disk. All components of the host magnetic field $\mathbf{B}_{\rm host}$ with their stochastic properties and radial profile (see [87–90]) should be taken into account in order to evaluate the transfer matrix $\mathcal{U}_2(\mathcal{E}; y_3, y_2)$, where $y_3$ denoted the radius of the external luminous edge of the galaxy. Photon-ALP conversion in the host turns out to be substantial.

*Photon-ALP oscillations in extragalactic space*—The present-day knowledge of the extragalactic magnetic field $\mathbf{B}_{\rm ext}$ is still very poor. While establishing an upper bound is a fairly simple task leading to $B_{\rm ext} < 1.7 \cdot 10^{-9}$ G with a coherence length $\mathcal{O}(1)$ Mpc [91], deriving a lower bound is a tricky business, since the result depends on the coherence length, on the variability of the measured sources of VHE gamma rays, on how long they are monitored, on their duty cycle and on the uncertainties of the induced cascades (a clear review of this topic is [92]). It is therefore not surprising that a large spread in the results exists, generally assuming a coherence length $\mathcal{O}(1)$ Mpc. Examples of the resulting bounds are in chronological order: $B_{\rm ext} > 3 \cdot 10^{-16}$ G (2010) [93], $B_{\rm ext} > 5 \cdot 10^{-15}$ G (2010) [94], $B_{\rm ext} > 10^{-15}$ G (2011) [95], $B_{\rm ext} > \mathcal{O}(10^{-16} \text{ to } 10^{-15})$ G for a source duty cycle of $\mathcal{O}(10^2 \text{ to } 10^4)$ yr (2011) [96], $B_{\rm ext} > 10^{-18}$ G for a very short source duty cycle of (3–4) yr, which can be larger by an order of magnitude if the intrinsic source flux above (5–10) TeV is large (2011) [97], $B_{\rm ext} < 0.3 \cdot 10^{-15}$ G or $B_{\rm ext} > 3 \cdot 10^{-15}$ G (2014) [98], $B_{\rm ext} > 10^{-14}$ G (2017) [99], and a very recent result is $B_{\rm ext} > 7.1 \cdot 10^{-16}$ G (2023) for a coherence length of 1 Mpc and a source duty cycle of 10 yr, which becomes $B_{\rm ext} > 1.8 \cdot 10^{-14}$ G and $B_{\rm ext} > 3.9 \cdot 10^{-14}$ G for a duty cycle of $10^4$ yr and $10^7$ yr, respectively [100].

Manifestly, the possibility of a very small $B_{\rm ext}$ cannot be excluded. Nevertheless, since about twenty years it has become customary to described $\mathbf{B}_{\rm ext}$ by means of a very specific model. It consists of a domain-like network, in which $\mathbf{B}_{\rm ext}$ is supposed to be homogeneous over a whole domain of size $L_{\rm dom}$ equal to its coherence length, with $\mathbf{B}_{\rm ext}$ changing randomly its direction from one domain to the next, keeping approximately the same strength. Therefore, the photon-ALP beam propagation becomes a *random process*, and only a single realization at once can be observed. In addition, it has always been assumed that such a change of direction is abrupt, because then the beam propagation equation is easy to solve [101,102]. Physically, such a scenario—called *domain-like sharp-edges* (DLSHE)—rests upon outflows from primeval galaxies further amplified by turbulence [103–106]. Common benchmark values are $B_{\rm ext} = \mathcal{O}(10^{-9})$ G on a coherence length $\mathcal{O}(1)$ Mpc which sets the value of $L_{\rm dom}$ (for more details, see [107]). In order to be definite, the authors of [83] have chosen $B_{\rm ext} \simeq 10^{-9}$ G, and $L_{\rm dom}$ in the range $(0.2 - 10)$ Mpc with $\langle L_{\rm dom} \rangle = 2$ Mpc. But the abrupt change in direction at the interface between two adjacent domains leads to a failure of the DLSHE model at the energies considered here. A way out of this difficulty is to smooth out the sharp edges of the domains, so that the components of $\mathbf{B}_{\rm ext}$ change continuously across the interface, thereby leading to the *domain-like smooth-edges* (DLSME) models, built up in [107,108]. Only the ALP scenarios described in [83,107,108] contemplate photon-ALP oscillations in extragalactic space within the DLSME models. As discussed in detail in [83], above energies of about 20 TeV photon dispersion on the CMB [109] makes the probability for photon-ALP oscillations vanishingly small. Accordingly $\mathcal{U}_3(\mathcal{E}; y_4, y_3)$ is computed, where $y_4$ is the position of the outer luminous edge of the Milky Way.

*Photon-ALP oscillations in the Milky Way*—Instrumental for our need are the morphology of the magnetic field $\mathbf{B}_{\rm MW}$ and of the electron number density $n_{{\rm MW},e}$ in the Galaxy. For $\mathbf{B}_{\rm MW}$ the model of Jansson and Farrar [110–112] is employed, which is more complete as compared to the one of Pshirkov et al. [113], even though no substantial differences are found by using the latter. Concerning $n_{{\rm MW},e}$, the model developed in [114] is used. The transfer matrix in the Milky Way $\mathcal{U}_4(\mathcal{E}; y_5, y_4)$—with $y_5$ denoting the position of the Earth—is evaluated as in Section 3.4 of [70]. Here, photon-ALP conversion is appreciable.

Just like in quantum mechanics, the overall transfer matrix from the source to the observer is the product of the ones evaluated in each of the above four regions, namely

$$\mathcal{U}(\mathcal{E}; y_5, y_1) = \prod_{i=1}^{4} \mathcal{U}_i(\mathcal{E}; y_{i+1}, y_i)\,. \tag{10}$$

Thanks to Equations (8) and (10) the photon survival probability from GRB 221009A to us can be evaluated as

$$P_{\rm ALP}(\mathcal{E}; \gamma \to \gamma) = \sum_{i=x,z} {\rm Tr}\left[\rho_i\, \mathcal{U}(\mathcal{E}; y_5, y_1)\, \rho_{\rm unp}\, \mathcal{U}^\dagger(\mathcal{E}; y_5, y_1)\right]\,, \tag{11}$$

where $\rho_x \equiv {\rm diag}(1,0,0)$, $\rho_z \equiv {\rm diag}(0,1,0)$, $\rho_{\rm unp} \equiv {\rm diag}(0.5, 0.5, 0)$. The result is plotted in Figure 1 and changes very little by assuming or neglecting an extragalactic magnetic field. Actually, Figure 1 shows that photons of $\mathcal{E} > 10\,\mathrm{TeV}$ observed by LHAASO are successfully explained within the ALP scenario. Thus, a *hint at new physics* emerges in the form of an ALP with the parameters space defined at the beginning of this Section.

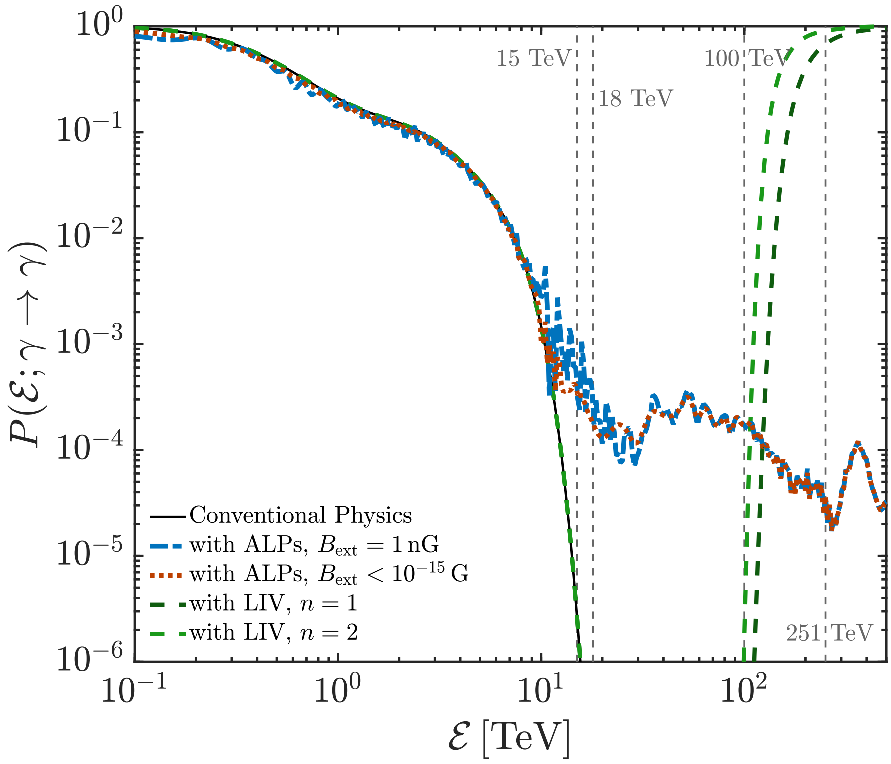


**Figure 1.** Photon survival probability $P(\mathcal{E}; \gamma \to \gamma)$ versus energy $\mathcal{E}$ within conventional physics, the ALP scenario (for $B_{\rm ext} = 10^{-9}$ G and $B_{\rm ext} \lesssim 10^{-15}$ G), and the LIV scenario (at leading order with $n = 1$ and also for $n = 2$). See text for more details. (Credit: [8]).

## 7. Second Challenge to Conventional Physics

Let us now address the photon at $\mathcal{E} = 300^{+43}_{-38}\,\mathrm{TeV}$ detected by the Carpet collaboration [17]. As shown in Figure 1, the photon survival probability in the presence of the considered ALPs at $\mathcal{E} = 300\,\mathrm{TeV}$ is considerably smaller than at $\sim$15 TeV, and so we expect that above this range ALPs fail to explain the event in question.

Actually, this conclusion can be made sharper by the following argument. As already stated, the Carpet collaboration estimated the *emitted* flux $\mathcal{F}_{\rm em}(\mathcal{E})$ which ultimately fits its photon, and finds that it is in order-of-magnitude consistent with the power-law one reported by the LHAASO collaboration (see Figure 2) as extrapolated to higher energies. Further, the observed flux can be written as

$$\mathcal{F}_{\rm obs}(\mathcal{E}) = \frac{dN_\gamma}{d\mathcal{E}\, dA\, dt} \,, \tag{12}$$

where $dN_\gamma$ is the number of photons observed in the energy range $d\mathcal{E}$ within the effective area $dA$ of the detector during the exposure time $dt$. Hence, by combining the first equality in Equation (2) (dropping CP and $z$) with Equation (12) we find

$$\frac{dN_\gamma}{d\mathcal{E}\, dA\, dt} = P(\mathcal{E}; \gamma \to \gamma)\, \mathcal{F}_{\rm em}(\mathcal{E}) \,. \tag{13}$$

For Carpet observation the energy range is $\Delta\mathcal{E} \simeq 81\,\mathrm{TeV}$, the effective detection area is $\Delta A \simeq 60\,\mathrm{m}^2$ and the exposure time is $\Delta t \simeq 1\,\mathrm{day}$. So—once $P(\mathcal{E}; \gamma \to \gamma)$ is given—from Equation (13) the expected number of observed photons $N_\gamma$ is obtained. Within *conventional physics* the evaluation of $P_{\rm CP}(\mathcal{E}; \gamma \to \gamma)$ is standard and Equation (13) gives $N_\gamma^{\rm CP} \sim 10^{-96}$! Within the *ALP scenario* Equation (13) yields $N_\gamma^{\rm ALP} \sim 10^{-5}$, to be contrasted with $N_\gamma^{\rm Carpet} \sim 1$. This shows that the ALPs considered above do *not* explain the Carpet photon.

Thus, a *new* kind of physics has to be looked for in order to get $N_\gamma^{\rm Carpet} \sim 1$, which has to be added to ALPs in such a way to retain the previous explanation of the LHAASO VHE photons and not to spoil that result.

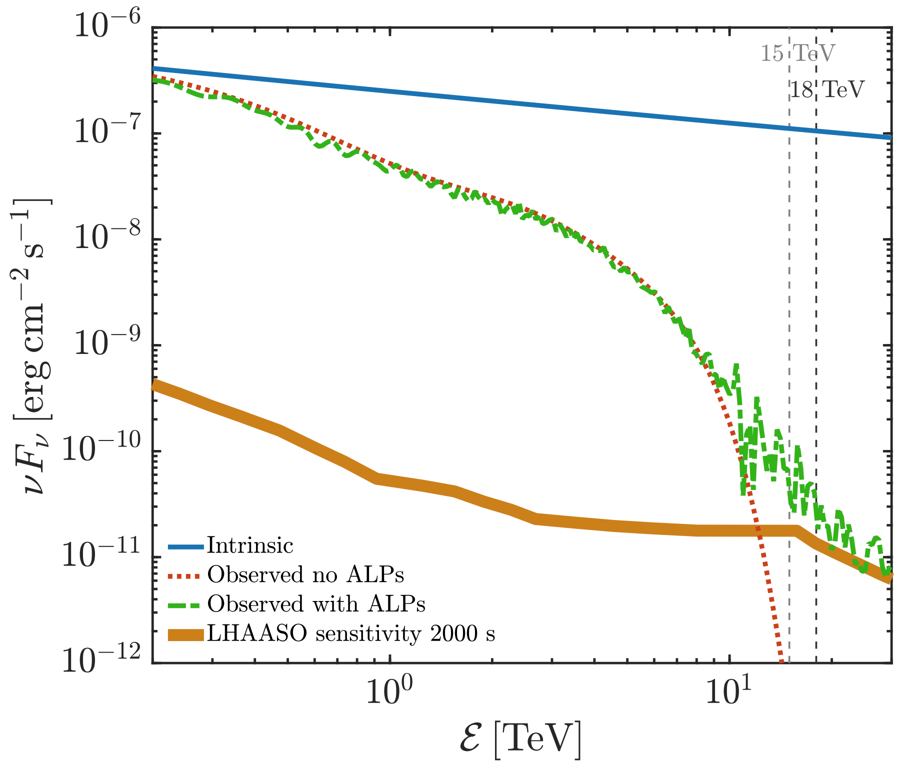


**Figure 2.** Observed SED versus energy $\mathcal{E}$ within conventional physics and the ALP scenario. Reported is also the LHAASO sensitivity and the emitted SED of GRB 221009A as measured by LHAASO [13,15], extended up to the Carpet energies [17], but shown here up to 30 TeV. (Credit: [8]).

## 8. Motivation for Lorentz Invariance Violation (LIV)

Global Lorentz invariance associated with the ISO (3,1) spacetime symmetry of special relativity is broken in general relativity and global Lorentz transformations are replaced with local ones, which are a particular case of general coordinate transformations. Consequently, the standard photon dispersion relation

$$p^2 = \mathcal{E}^2 \tag{14}$$

becomes $g_{\mu\nu}(x)\, p^\mu p^\nu = 0$ in general relativity, as well as in generic cosmological models. However, observational evidence such as the analyses of the Cosmic Microwave Background (CMB) [115–117], the baryon acoustic oscillations (BAO) [118–120], and the large-scale structure power spectra [121] indicate that our Universe is spatially flat to a high precision. Theoretically, inflationary cosmology further supports spatial flatness [122–124].

Therefore, light propagation throughout our specific Universe is governed by the dispersion relation $g_{\mu\nu}(t)\, p^\mu p^\nu = 0$ and so in the *local Universe*—say, for $z < 0.2$—the special relativistic relation Equation (14) still describes the propagation of light rays. Nevertheless, as already pointed out LIV has been recognized since many years as a low-energy effect of quantum gravity, whose energy scale is the Planck mass $M_P \simeq 1.22 \cdot 10^{19}$ GeV. A characteristic feature of quantum gravity is that spacetime is *not* a fixed framework wherein a system behaves but becomes just the *dynamical system* governed by it. While this occurs around $M_P$, the goal of LIV theories is to capture the low-energy manifestations of this dynamical spacetime which is characterized by a LIV scale $\mathcal{E}_{\rm LIV}$ expected to be not too far from $M_P$ [125–132]. One of these low-energy manifestations is the deformation of the dispersion relation Equation (14), and a suitable parametrization is

$$p^2 = \mathcal{E}^2 \left[ 1 + f\left( \frac{\mathcal{E}}{\mathcal{E}_{\rm LIV}} \right) \right] , \tag{15}$$

where $f(\cdot)$ is a model-dependent smooth function such that $f(0) = 0$ since it has to vanish as $\mathcal{E}_{\rm LIV} \to \infty$. At presently accessible energies $\mathcal{E} \ll \mathcal{E}_{\rm LIV}$ the same approach used in effective field theories can be applied to the deformed dispersion relation Equation (15)—rather than to the Lagrangian—thereby leading to

$$p^2 = \mathcal{E}^2 \left[ 1 + \xi \, \frac{\mathcal{E}}{\mathcal{E}_{\rm LIV}} + \xi \left| \mathcal{O}\left( \frac{\mathcal{E}^2}{\mathcal{E}_{\rm LIV}^2} \right) \right| \right] \tag{16}$$

with $\xi = 1$ for subluminal photon propagation and $\xi = -1$ for superluminal photon propagation. Moreover, only the first nonvanishing power of $\mathcal{E}/\mathcal{E}_{\rm LIV}$ has to be retained in Equation (16). Such modification affects both the quantum mechanical propagators and the reaction thresholds, notably concerning the $\gamma\gamma \to e^+e^-$ process [133–136]. What happens is that for subluminal propagation VHE photons from cosmological sources interact with EBL photons at *higher* energies, where the EBL density turns out to be *smaller*. Therefore, this effect *increases* the cosmic transparency to VHE photons, quantitatively described by an enhanced photon survival probability $P_{\rm LIV}(\mathcal{E})$ [137–139]. Accordingly, subluminal LIV scenarios *may* provide a natural explanation for the 300 TeV Carpet photon.

Before proceeding, we stress that Equation (16) further implies that photons acquire an energy-dependent time of flight [125,131]. In particular, for subluminal propagation photons are affected by a *time delay* (the explicit equation for the time delay appropriate to the cosmological context has been derived in [140]).

Coming back to our main line of reasoning, in order to see whether the above guess is correct we focus our attention on Equation (16) at first and second order in $\mathcal{E}/\mathcal{E}_{\rm LIV}$. And to derive $\mathcal{E}_{\rm LIV}$ in both cases it might be tempting to still resort to Equation (13) but differently than what was previously done. Now, $N_\gamma \sim 1$ must be set and $P_{\rm ALP+LIV}(\mathcal{E}; \gamma \to \gamma)$ should be used, as discussed in [9] where the full treatment of the ALP + LIV scenario is presented. Accordingly, at Carpet energies $P_{\rm ALP+LIV}(\mathcal{E}; \gamma \to \gamma)$ is plotted in Figure 1 with the dark green dashed line representing the photon dispersion relation modified by LIV at first order ($n = 1$). The case $n = 2$ in Figure 1—represented by the light green dashed line—corresponds to the second-order term in Equation (16), under the assumption that the first order term vanishes. Manifestly, LIV effects start to dominate over ALP ones for $\mathcal{E} \gtrsim 150\,{\rm TeV}$, so that the LIV alone component reported in Figure 1 is a viable way to apply the ALP + LIV scenario around the Carpet energies.

However—while the above results are fully correct—the outlined procedure to estimate $\mathcal{E}_{\rm LIV}$ would be too naive, since only a single photon has been detected. Because of this fact, the Poisson statistics has to be employed. The details of this approach can be found in [9] and here we merely report the results. In $n = 1$ non-birefringent LIV [126] the upper bound on the LIV scale to get $N_\gamma \simeq 1$ is $\mathcal{E}_{\rm LIV} < 1.22 \cdot 10^{21}$ GeV at the $2\sigma$ level, but—assuming that the first-order term vanishes—in $n = 2$ LIV the upper bound becomes $\mathcal{E}_{\rm LIV} < 2.03 \cdot 10^{13}$ GeV at the $2\sigma$ level [9] (all this is consistent with current bounds [141–145]).

Before closing this Section a remark is compelling. The aim of [9] was to investigate the possibility that a photon of $E \sim 300\,{\rm TeV}$ can reach us from a redshift $z = 0.151$: this is the *first puzzle*. An 'open minded strategy' has been adopted to make *no assumption* about either the emission mechanism or the reason why the Carpet photon arrived so late as compared to the LHAASO photons. This attitude was motivated in general by the fact that GRB 221009A is so much different from any other known GRB, and in particular from the power-law emitted spectrum considered above (more about this, in Section 9). Nevertheless, understanding why the Carpet photon had a time delay of more than one hour as compared to the LHAASO photons is a crucial issue: this is the *second puzzle*. Very recently—assuming that GRB 221009A behaves in a fashion very similar to all other GRBs—Ofengeim and Piran reached the conclusion that the second puzzle is solved provided that LIV is described by Equation (16) at *second-order* ($n = 2$) (namely assuming that the first order term vanishes) finding $\mathcal{E}_{\rm LIV} = 1.30^{+0.56}_{-0.35} \cdot 10^{-7}\, M_P \simeq 1.59 \cdot 10^{12}$ GeV [146]. Quite remarkably, this result is *consistent* with the previous one.

## 9. Discussion

So far, we have discussed the first ALP + LIV scenario appeared in the literature to explain the observability of the photons detected both by LHAASO and by Carpet [8,9]. We emphasize that the specific ALPs considered so far are not *ad hoc*, since they previously unfolded two astrophysical puzzles in a natural fashion, as we shall see below. However, some preliminaries are required.

About 10% of active galactic nuclei (AGNs) have two jets along opposite directions. When one of them occasionally points towards us the AGN is called *blazar*. Their VHE gamma rays up to $\mathcal{O}(1)$ TeV are produced close to the central engine—a supermassive black hole (SMBH)—in two alternative ways. One is the *synchrotron self-Compton* (SSC) mechanism, wherein photons at low energies arise from the synchrotron emission of accelerated electrons, and are next upscattered to the VHE band by the inverse Compton effect on the parent electrons as they propagate inside the jets [147–149] (sometimes also external photons are needed). Alternatively, VHE photons can arise from hadronic interactions along with pions and neutrinos [150,151]. Remarkably, both emission models predict emitted spectra which—to a good approximation and for almost all blazars—have a single power law behaviour $\mathcal{F}_{\rm em} = K_{\rm em}\, E^{-\Gamma_{\rm em}}$, where $K_{\rm em}$ is the normalization and $\Gamma_{\rm em}$ is the *emitted slope*. Note that in general $\mathcal{F}_{\rm em}$ varies with time, in which case a blazar is said to be *flaring*. There are two kinds of blazars: (1) *BL Lacs*, (whose name comes from the first observed one, BL Lacertae) which lack thermal features like broad emission lines in their optical spectra and whose jets extend out to about 1 kpc, and (2) *Flat spectrum radio quasars* (FSRQs)—which are like the first quasars discovered in 1963—whose jets extend out to about 1 Mpc. Their characteristic feature are the luminous broad optical emission lines flagging the existence of photoionized clouds rapidly rotating around the central SMBH and organized in the so-called *broad line region* (BLR)—which is therefore rich of ultraviolet photons—extending out to (6–9)$\cdot 10^{17}$ cm from the centre. Therefore, the VHE photons produced at the jet base undergo the same $\gamma\gamma \to e^+e^-$ process considered in Section 4 with the EBL replaced with the BLR. As a result, according to conventional physics *only* photons of energy up to (10–20) GeV are emitted [152–154].

We are now in a position to discuss in chronological order three hints at an ALP with $m_a = \mathcal{O}(10^{-10})$ eV and $g_{a\gamma\gamma} = \mathcal{O}(10^{-12})$ GeV$^{-1}$.

*First hint*—Owing to the above discussion, the observation of FSRQs at TeV energies gave rise to a big surprise [155–157]. The most striking case was PKS 1222 + 216 at $z = 0.432$ observed simultaneously by Fermi/LAT in the range $\mathcal{E} =$ (0.3–3) GeV [158] and by MAGIC in the band $\mathcal{E} =$ (70–400) GeV [157]. Moreover, MAGIC detected a flux doubling in about 10 min which entails that the emitting object has size of $\sim 10^{14}$ cm, but its observed flux is similar to that of a whole BL Lac. So, there are two problems at once!

Various astrophysical explanations have been put forward, but all of them are totally *ad hoc*. Perhaps, the simplest but most extravagant one amounts to suppose that a very small emitting blob of size $\sim 10^{14}$ cm is located beyond the BLR, namely at a distance larger $\sim 10^{18}$ cm from the centre! Moreover, this proposal is very difficult to implement within the standard blazar model [159–161]. An alternative option which instead naturally fits inside the standard blazar model consists in the introduction of an ALP with values of $m_a$ and $g_{a\gamma\gamma}$ in the previous range. Accordingly—much in the same way as VHE extragalactic photons partially survive the EBL absorption thanks to photon-ALP oscillations—here VHE photons produced close to the jet base partially circumvent the BLR absorption owing to photon-ALP oscillations in the jet magnetic field. Quite remarkably, a very detailed analysis has shown that the SED predicted by this model turns out to be in very good agreement with the observed one [66].

*Second hint*—Let us consider the most homogeneous sample of VHE flaring BL Lacs whose following properties should be known: the redshift $z$, the observed spectrum with error bars, the energy range $\Delta\mathcal{E}(z)$ wherein every one is observed, and $z < 0.6$. This analysis was done in 2019, and at that time only 39 BL Lacs were found to obey these requirements, forming the sample $\mathcal{S}$. Then, a deceptively simple question was addressed, concerning a possible *statistical correlation* between the emitted slope *distribution* $\{\Gamma_{\rm em}(z)\}$ of the elements of $\mathcal{S}$ and their *redshift* $z$.

In order to see what happens, the observed flux $\mathcal{F}_{\rm obs}(\mathcal{E}, z)$ of each BL Lac in $\mathcal{S}$ was EBL-deabsorbed according to Equation (2) where $\tau_{\rm CP}(\mathcal{E}, z)$ has been computed from the EBL model of [162]. In this way, for *every* BL Lac in $\mathcal{S}$ at redshift $z$ the emitted slope $\Gamma^{\rm CP}_{\rm em}(z)$ was inferred starting from the observed one $\Gamma_{\rm obs}(z)$ according to conventional physics. Next, a statistical analysis of the $\{\Gamma^{\rm CP}_{\rm em}(z)\}$ has been performed. Using the least square method all $\Gamma^{\rm CP}_{\rm em}(z)$ have been fitted with 1, 2, 3 parameters, and the corresponding $\chi^2_{\rm red}$ has been evaluated. Since the minimal value of $\chi^2_{\rm red}$ selects the 3 parameter case, the resulting the best-fit regression line is a *concave parabola* in the $\Gamma_{\rm em} - z$ plane decreasing as $z$ increases, thereby implying that BL Lacs with harder spectra are found on average at larger redshifts. This conclusion implies a *statistical correlation* between the $\{\Gamma^{\rm CP}_{\rm em}(z)\}$ distribution and $z$: this issue is called *spectral anomaly*.

Why should such a statistical correlation exist? Certainly evolutionary effects in the BL Lacs are harmless for $z < 0.6$, and when all observational selection biases are taken into account the correlation in question looks physically mysterious. Indeed, if it existed it would mean that some unknown effect told a source at e.g., $z = z_1$ what $\Gamma^{\rm CP}_{\rm em}(z_1)$ should be, knowing for instance $\Gamma^{\rm CP}_{\rm em}(z_2)$. Instead, the natural expectation is that the best-fit regression line of the $\{\Gamma_{\rm em}(z)\}$ distribution should be a *straight horizontal* line in the $\Gamma_{\rm em} - z$ plane.

As a way out of this conundrum, ALPs have been put into the game, assuming the existence of a fairly strong extragalactic magnetic field described by the same domain-like network considered in Section 6. By repeating the above statistical analysis for $m_a = \mathcal{O}(10^{-10})$ eV and $2.94 \cdot 10^{-12}$ GeV$^{-1}$ $< g_{a\gamma\gamma} < 0.66 \cdot 10^{-10}$ GeV$^{-1}$ it turned out that the best-fit regression line is exactly *straight* and *horizontal* in the $\Gamma_{\rm em} - z$ plane. Besides elegantly getting rid of the spectral anomaly, this result looks astonishing. Of course, by changing the effective level of EBL absorption the $z$-dependence of the best-fit regression line of the $\{\Gamma^{\rm ALP}_{\rm em}(z)\}$ distribution is expected to differ from that of the $\{\Gamma^{\rm CP}_{\rm em}(z)\}$ distribution. As a consequence, its shape in the $\Gamma_{\rm em} - z$ plane changes as well. But to become exactly straight and horizontal, which is the *only possibility*—out of infinitely-many ones—in agreement with the physical expectation looks really amazing [71].

*Third hint*—This is just the ALP-induced observability of GRB 221009A at $\mathcal{E} > 10$ TeV discussed in detail in Section 6 [8].

Overall, we have three independent hints—arising from very different astrophysical situations—at an ALP with $m_a = \mathcal{O}(10^{-10})\,\mathrm{eV}$ and $g_{a\gamma\gamma} = \mathcal{O}(10^{-12})\,\mathrm{GeV}^{-1}$.

Needless to say, after the appearance of the ALP + LIV proposal [8,9] various different models have been developed in order to explain either the observability of GRB 221009A or the generation of its emitted photons. Below, we shortly review some of them which we regard as the most representatives, without claiming to be complete. Moreover, our discussion will be schematic and rather brief.

**ALP models:** Owing to the great interest in ALPs, several authors have employed them in order to unfold the LHAASO results, following basically the same strategy first implemented in [8] with some variations in the ALP parameters, in the GRB 221009A characteristics and in the computational methods. But there is a general agreement that ALPs cannot explain the updated Carpet result [163–169]. In [170] a model with the ALPs arising in the non-perturbative context of a first-order phase transition has been put forward, and in [171] a detailed discussion of the parameters of GRB 221009A has been carried out in the ALP context, but in either case the MWD bound [84] fails to be met. The same criticism also applies to [172], in which a new probabilistic method has been employed to constrain all model parameters.

**Scalar model:** At variance with ALPs which are pseudo-scalar particles, a model based on a new singlet scalar particle has been proposed in [173]. This scalar mixes with the standard model particles through a Higgs coupling. Hence it is expected to be copiously produced in GRB 221009A. If its lifetime is such that it decays into two photons fairly close to the Milky Way, these photons are basically unaffected by the EBL and can account for the LHAASO observations.

**Neutrino models:** As a preliminary step, we stress that it has been strongly suggested that GRB 221009A should be a source of ultra-high-energy cosmic rays [174–176]. In the search for a mechanism which decreases the EBL absorption of the highest energy photons detected by LHAASO, two models involving neutrinos have been put forward.

*First model*—The existence of a new heavy neutrino $N$ with mass $\sim 0.1\,\mathrm{MeV}$ is assumed, which mixes with pions and kaons emitted by GRB 221009A (in agreement with the above statement). Further, $N$ couples to ordinary neutrinos but not to leptons. Finally, the radiative decay $N \to \nu + \gamma$ is supposed to occur rather close to the Galaxy so that the produced photons can propagate almost unhindered to us. However, besides the existence of $N$ also the radiative decay in question requires an extension of the Standard Model [177].

*Second model*—An alternative possibility that has been investigated involves—as a first step—the high-energy neutrinos produced in hadronic interaction (as already stated, ultra-high-energy hadrons are expected to be emitted by GRB 221009A). As these neutrinos propagate they are supposed to scatter off the cosmic neutrino background, producing in this way ALPs through the reaction $\nu + \nu \to a + a$, where $a$ denotes an ALP. So, besides the existence of ALPs also a dimension-five operator $a^2\,\nu^T\,\nu$ must be added to the Standard Model. The last step consists in the ALP conversion into photons in the magnetic field of the Milky Way. An even more complex scenario requires the existence of two different kinds of ALPs $a$ and $a'$ produced in the reaction $\nu + \nu \to a + a'$ [178].

Note that the observability problem for the Carpet photon is left unsolved by all models considered so far.

**Conventional physics models:** Three scenarios which do not involve any new physics aiming to explain the VHE photon emission from GRB 221009A have been suggested, which we summarize below.

*Electron and proton synchrotron models*—Although the theoretical modeling of the emission mechanisms for the photons detected by LHAASO are always carried out within the relativistic fireball scenario, they differ in some details and this is a matter of great debate. The production of VHE photons in GRBs during the afterglow has repeatedly been discussed in terms of the SSC mechanism (the early applications of the SSC mechanism to GRBs can be found in [179–182]). In particular, some authors claim that the standard SSC mechanism is able to account for *all* photons emitted during the afterglow of GRB 221009A (see for instance [183]). Alternatively, other researches argue that only photons up to $\mathcal{O}(1)\,\mathrm{TeV}$ can be generated in this way and next be upscattered by the *external* inverse Compton (EIC) [184–186]. However, some people believe that because of the Klein-Nishina effect the SSC model falls short at producing photons of energies considerably larger than $\mathcal{O}(1)\,\mathrm{TeV}$, thereby failing to explain the highest energy photons observed by LHAASO. An alternative possibility to generate higher energy photons is the *proton synchrotron* (PS) mechanism—with electrons replaced with protons—which has the advantage to easily produce photons of energies $\mathcal{O}(10)\,\mathrm{TeV}$ [187]. Quite recently—within the *reverse shock* model of GRBs [187–189]—a two-episode strategy has been proposed [190]: the first takes place during the prompt emission while the second occurs during the afterglow [191]. In the first episode only photons of energies up to $\mathcal{O}(1)\,\mathrm{GeV}$ are emitted by the SSC and EIC mechanisms, whereas in the second episode photons of energy up to $\mathcal{O}(10)\,\mathrm{TeV}$ are generated by the PS mechanism, hence explaining the highest energy LHAASO photons. But the observability issue of the detected highest energy photons remains totally unsolved not only for LHAASO but also for Carpet.

*Proton beam model*—Regardless of any GRB, between 2010 and 2012 a new scenario has been developed by Kusenko and collaborators as an alternative to the SSC emission mechanism invoked to explain the VHE photons detected from blazars. Specifically, a collimated beam of ultra-relativistic protons is accelerated in the jet and interacts with extragalactic background photons thereby producing electromagnetic cascades [192–194]. Because secondary photons generated in the cascades are expected to be emitted close to the Earth, they suffer a reduced EBL absorption, resulting in a hardening of the observed blazar spectra. Needless to say, the extragalactic magnetic field must be close to the lower bounds quoted in Section 6 in order not to spread the proton beam.

Very recently, this approach has been applied to GRB 221009A with the goal to explain the photons of $\mathcal{E} > 10\,\mathrm{TeV}$ detected by LHAASO in terms of conventional physics, thereby getting rid of the more exotic ALP scenario [195] (the authors include also the LIV scenario, but as shown in [8,9] and in Figure 1 it does not work). A key-assumption is that the extragalactic magnetic field obeys the upper bound $B_{\rm ext} < 10^{-16}\,\mathrm{G}$. As emphasized by the authors, besides accounting for the photon spectrum observed by LHAASO the secondary photons must be detected during the time lapse of $2000\,\mathrm{s}$, which is the time window of LHAASO for *all* detected photons of any energy. Magnetic fields are known to bring about *time delays* in the protons—which obviously show up in the observed photons—and three contributions should be taken into account: (1) $\Delta t_{\rm host}$ caused by the host galaxy magnetic field $\mathbf{B}_{\rm host}$, (2) $\Delta t_{\rm ext}$ arising from the extragalactic magnetic fled $\mathbf{B}_{\rm ext}$, and (3) $\Delta t_{\rm casc}$ from the magnetic field $\mathbf{B}_{\rm casc}$ in the electromagnetic cascade. Overall, the constraint reads $\Delta t_{\rm host} + \Delta t_{\rm ext} + \Delta t_{\rm casc} < 2000\,\mathrm{s}$. According to the authors, the host galaxy is a spiral with a central regular magnetic field $B_{\rm host} \sim 1\,\mu\mathrm{G}$ smoothly decreasing as the galactocentric distance increases, with correlation length $L_{\rm host} \sim 10\,\mathrm{pc}$. Additionally, it is claimed that the location of GRB 221009A is uncertain, and by analogy with other galaxies hosting a GRB [196–198] the position of GRB 221009A is taken inside a star forming region in the spiral arms at the outskirts of the host on the side of the observer, where the regular magnetic field is assumed to be significantly lower than $1\,\mu\mathrm{G}$. An unquantified turbulent magnetic field is supposed to exist in the star forming region encompassing GRB 221009A. Finally, the proton beam has energy $\mathcal{E} \sim 10^5\,\mathrm{TeV}$ and it is assumed to cross a distance inside the host equal to $d_{\rm host} \sim 0.1\,\mathrm{kpc}$, typical of the disk thickness. Because $\Delta t_{\rm host}$ is given by [195,199]

$$\Delta t_{\rm host} \sim 400 \left( \frac{d_{\rm host}}{\rm kpc} \frac{L_{\rm host}}{10\,\rm pc} \right)^{3/2} \left( \frac{B_{\rm host}}{\mu\rm G} \frac{10^5\,\rm TeV}{\mathcal{E}} \right)^2 \,\mathrm{s}\,, \tag{17}$$

the authors conclude that $\Delta t_{\rm host}$ is indeed smaller than 2000 s.

We call such a scenario into question. We start by recalling the lower bounds on the extragalactic magnetic field reported in Section 6, and upon comparison of the upper bound $B_{\rm ext} < 10^{-16}\,\mathrm{G}$ of this model we see that for some lower bounds there is an agreement but for others there is a disagreement, with uncontrolled uncertainties. So, the application of the proton beam model to GRB 221009A stands on an uncertain basis. A more severe criticism is as follows. Both HST and JWST have shown that GRB 221009A is located at about 0.65 kpc from the centre of a star forming spiral galaxy seen nearly edge-on [85,86]. Therefore, GRB 221009A is close to the host centre and *not* in its outskirts. In addition, emission lines of $H_2$—which trace dense star forming regions—have been detected from several patches of the host but the strongest ones from the site of GRB 221009A, and the star-formation-rate is $\mathrm{SFR} = 0.17\,M_\odot/\mathrm{yr}$ [86]. Hence, the host is likely to be a rather normal spiral. Moreover, the stellar mass of the host has been estimated as $M_{{\rm host},*} \simeq 3.72 \cdot 10^9\,M_\odot$ [86], while the host stellar radius $\mathcal{R}_{{\rm host},*}$ is unknown. However, given the fact that the Milky Way stellar radius is $\mathcal{R}_{{\rm MW},*} \simeq 25\,\mathrm{kpc}$ and $M_{{\rm host},*}/M_{{\rm MW},*} \simeq 3.72 \cdot 10^9\,M_\odot/(8.1 \cdot 10^{10}\,M_\odot) \simeq 4.6 \cdot 10^{-2}$ we argue that $\mathcal{R}_{{\rm host},*} \simeq 10\,\mathrm{kpc}$. As a consequence—since the host is seen nearly edge-on—we conclude that *effectively* the line of sight to GRB 221009A lies inside the disk of the host for *at least* $d_{\rm host} \simeq 6\,\mathrm{kpc}$, which is larger by a factor of $\sim$60 than the value $d_{\rm host} \sim 0.1\,\mathrm{kpc}$ used in this model. Let us turn to the regular magnetic field. What matters for us is its behaviour in the disk (starting from the centre), which is almost universal in normal spiral galaxies, with $B_{\rm disk} \sim 1\,\mu\mathrm{G}$ and correlation length $L_{\rm host} \sim 1\,\mathrm{kpc}$ according to the literature [200–204]. But in order to be conservative we take its average value inside the disk as $\langle B_{\rm host,disk} \rangle \sim 0.1\,\mu\mathrm{G}$. Putting everything together, Equation (17) gives $\Delta t_{\rm host} \sim 6 \cdot 10^4\,\mathrm{s}$, which exceed the LHAASO window by a factor of $\sim$30. Thus, the proton beam model fails to explain most of the photons observed by LHAASO. But our result is stronger than that. As repeatedly stressed, the observability issue for LHAASO concerns only photons of $\mathcal{E} > 10\,\mathrm{TeV}$, and we recall from Section 3 that the LHAASO time window for photons of $\mathcal{E} > 3\,\mathrm{TeV}$ is only 670 s. So, to solve the problem it is necessary that $\Delta t_{\rm host} < 670\,\mathrm{s}$, whereas we find $\Delta t_{\rm host} \sim 6 \cdot 10^4\,\mathrm{s}$, having taken a conservative attitude (note that we have neglected the random magnetic field in the disk since it would exacerbate our result). In conclusion, a more careful rephrasing of the proton beam model as applied to GRB 221009A shows that such a model is doomed to failure.

ALPs are indeed compelling!

*Neutron beam model*—This scenario has first been proposed in [205] and further considered in [17] as an explanation of the Carpet photon. The basic idea is schematically as follows. During the GRB prompt emission phase, protons are accelerated to $\mathcal{E} > 10^3\,\mathrm{TeV}$ in the observer frame and efficiently interact with the strong surrounding photon field, producing gamma rays, $e^+e^-$ pairs, neutrinos and neutrons. These neutrons next interact with the interstellar matter of the star-forming region of the host galaxy encompassing the GRB generating (among other particles) a flux of ultra-relativistic $e^+e^-$ pairs and neutrinos. Electrons and positrons produce in turn the observed multi-TeV photons via synchrotron emission in the magnetic field of the host galaxy. This energy can be boosted by 1 order of magnitude either for a host magnetic field larger by a factor of 10 than usually assumed, or for an energy of the accelerated protons larger by a factor of (3–4) than generally supposed. By and large, photons of energy $\sim 100\,\mathrm{TeV}$ can be attained according to [17]. In addition, it is claimed that the time delay of the Carpet photon comes from the angular spread of the neutron beam. Further, we have seen that neutrinos are produced in the interaction of neutron with matter in the host and around it, and—as shown in [205]—the resulting neutrino flux has a multi-TeV energy and its strength is comparable to that of the gamma-ray flux. But the upper bound from IceCube [206,207] forces this flux to be smaller by an order of magnitude than the GRB 221009A VHE fluence (this criticism and some additional one can be found in [146]). Thus, the neutron beam model seems unable to explain the Carpet photon.

**LIV features:** In addition to the already quoted LIV constraints [141–145], further information from GRB 221009A concerning LIV have been derived in [146,208–212]. Note that all these papers but the last one pertain to the LHAASO observations.

## 10. Conclusions

The observation of GRB 221009A represents a breakthrough for both fundamental physics and VHE astrophysics. Indeed, nobody could expect to observe photons emitted by a GRB at $z = 0.151$ of energies above $10\,\mathrm{TeV}$ for any reasonable emission model due to the EBL absorption. Yet, GRB 221009A has been detected by LHAASO up to $\sim 15\,\mathrm{TeV}$ and by Carpet even up to $\sim 300\,\mathrm{TeV}$. Therefore, conventional photon propagation and standard explanations for the observation of this GRB are extremely challenged. As a consequence, new physics scenarios have been invoked in order to justify this revolutionary detection. We have reviewed in some detail the first self-consistent $\mathrm{ALP} + \mathrm{LIV}$ model for the observation of GRB 221009A, in which a not *ad hoc* ALP with mass $m_a = \mathcal{O}(10^{-10})\,\mathrm{eV}$ and two photon coupling $g_{a\gamma\gamma} = \mathcal{O}(10^{-12})\,\mathrm{GeV}^{-1}$ accounts for the observability of the LHAASO events above $10\,\mathrm{TeV}$ [8], whereas second-order ($n = 2$) LIV with $\mathcal{E}_{\mathrm{LIV}} = 1.30^{+0.56}_{-0.35} \cdot 10^{-7}\,M_P \simeq 1.59 \cdot 10^{12}\,\mathrm{GeV}$ explains both the observability of the Carpet event [9] and its time delay [146]. Moreover, we have shown that all alternative models aiming to explain the observability of the highest energy photons from GRB 221009A are either *ad hoc* or incorrect.

What remains to be understood is the emission mechanism for the highest energy observed photons, which is the *third puzzle* raised by GRB 221009A.

As far as ALPs are concerned, current and new observatories such as ASTRI Mini Array [213], CTAO [214], GAMMA-400 [215], HAWC [216], HERD [217], LHAASO [218], TAIGAHiSCORE [219], ALPS II [220], IAXO [221], STAX [222], ABRACADABRA [223] and the techniques developed by Avignone and collaborators [224–226] will be able to provide new information confirming or disproving the three hints at a very specific ALP reported in this review.

## Author Contributions

All authors have read and agreed to the published version of the manuscript.

## Funding

The work of G.G. is supported by a contribution from Grant No. ASI-INAF 2023-17-HH.0 and by the INAF Mini Grant 'High-energy astrophysics and axion-like particles', PI: G.G. The work of M.R. is supported by an INFN grant.

## Data Availability Statement

Data are available from the authors upon reasonable request.

## Acknowledgments

We thank Gabriele Ghisellini and Giovanni Pareschi for very useful discussions.

## Conflicts of Interest

The authors declare no conflict of interest.

## Use of AI and AI-Assisted Technologies

No AI tools were utilized for this paper.

## References

1. de Ugarte Postigo, A.; Izzo, L.; Pugliese, G.; et al. GRB 221009A: Redshift from X-shooter/VLT. *GRB Coord. Netw. Circ. Serv.* **2022**, *32648*, 1.
2. Castro-Tirado, A.J.; Sanchez-Ramirez, R.; Hu, Y.D.; et al. GRB 221009A: 10.4 m GTC spectroscopic redshift confirmation. *GRB Coord. Netw. Circ. Serv.* **2022**, *32686*, 1.
3. Malesani, D.B.; Levan, A.J.; Izzo, L.; et al. The brightest GRB ever detected: GRB 221009A as a highly luminous event at $z = 0.151$. *Astron. Astrophys.* **2025**, *701*, 134.
4. Williams, M.A.; Kennea, J.A.; Dichiara, S.; et al. [SWIFT Collaboration]. GRB 221009A: Discovery of an Exceptionally Rare Nearby and Energetic Gamma-Ray Burst. *Astrophys. J. Lett.* **2023**, *946*, L24.
5. Lesage, S.; Veres, P.; Briggs, M.S.; et al. [Fermi Collaboration]. Fermi-GBM Discovery of GRB 221009A: An Extraordinarily Bright GRB from Onset to Afterglow. *Astrophys. J. Lett.* **2023**, *952*, L42.
6. Axelsson, M.; Ajello, M.; Arimoto, M.; et al. [Fermi Collaboration]. GRB 221009A: The B.O.A.T. Burst that Shines in Gamma Rays. *Astrophys. J. Suppl.* **2025**, *227*, 24.
7. Burns, E.; Svinkin, D.; Fenimore, E.; et al. GRB 221009A: The BOAT. *Astrophys. J. Lett.* **2023**, *946*, L31.
8. Galanti, G.; Nava, L.; Roncadelli, M.; et al. Observability of the Very-High-Energy Emission from GRB 221009A. *Phys. Rev. Lett.* **2023**, *131*, 251001.
9. Galanti, G.; Roncadelli, M. Is Lorentz invariance violation found? *arXiv* **2025**, arXiv:2504.01830.
10. Piran, T. Gamma-ray bursts and the fireball model. *Phys. Rep.* **1999**, *314*, 575.
11. Piran, T. The physics of gamma-ray bursts. *Rev. Mod. Phys.* **2004**, *76*, 1143.
12. Nava, L. Gamma-ray Bursts at the Highest Energies. *Universe* **2021**, *7*, 503.
13. Cao, Z; Aharonian, F.; An, Q. [LHAASO Collaboration]. Very high-energy gamma-ray emission beyond 10 TeV from GRB 221009A. *Science Adv.* **2023**, *9*, eadj2778.
14. Huang, Y.; Hu, S.; Chen, S.; et al. [LHAASO Collaboration]. LHAASO observed GRB 221009A with more than 5000 VHE photons up to around 18 TeV. *GRB Coord. Netw. Circ. Serv.* **2022**, *32677*, 1.
15. Cao, Z.; Aharonian, F.; An, Q.; et al. [LHAASO Collaboration]. A tera–electron volt afterglow from a narrow jet in an extremely bright gamma-ray burst. *Science* **2023**, *380*, adg9328.
16. Dzhappuev, D.D.; Afashokov, Y.Z.; Dzaparova, I.M.; et al. [Carpet-2 Collaboration]. Swift J1913.1 + 1946/GRB 221009A: Detection of a 250-TeV photon-like air shower by Carpet-2. *ATEL* **2022**, *15669*, 1.
17. Dzhappuev, D.D.; Dzaparova, I.M.; Dzhatdoev, T.A.; et al. [Carpet-3 Collaboration]. Carpet-3 detection of a photonlike air shower with estimated primary energy above 100 TeV in a spatial and temporal coincidence with GRB 221009A. *Phys. Rev. D* **2025**, *111*, 102005.
18. Dwek, E.; Krennrich, F. The extragalactic background light and the gamma-ray opacity of the universe. *Astropart. Phys.* **2013**, *43*, 112.
19. Breit, G.; Wheeler, J.A. Collision of two light quanta. *Phys. Rev.* **1934**, *46*, 1087.
20. Heitler, W. *The Quantum Theory of Radiation*; Oxford University Press: Oxford, UK, 1960.
21. Nikishov, A. Absorption of high energy photons in the universe. *Sov. Phys. JETP* **1962**, *14*, 393.
22. Gould, R.J.; Schreder, G.P. Pair production in photon-photon collisions. *Phys. Rev.* **1967**, *155*, 1404.
23. Fazio, G.G.; Stecker, F.W. Predicted High Energy Break in the Isotropic Gamma Ray Spectrum: A Test of Cosmological Origin. *Nature* **1970**, *226*, 135.
24. Stecker, F.W.; De Jager, O.C.; Salamon, M.H. TeV gamma rays from 3C 279: A possible probe of origin and intergalactic infrared radiation fields. *Astrophys. J.* **1992**, *390*, L49.
25. Stecker, F.W.; Scully, S.T.; Malkan, M.A. An Empirical Determination of the Intergalactic Background Light from UV to FIR Wavelengths Using FIR Deep Galaxy Surveys and the Gamma-Ray Opacity of the Universe. *Astrophys. J.* **2016**, *827*, 6.
26. Saldana-Lopez, A.; Domínguez, A.; Pérez-González, P.G.; et al. An observational determination of the evolving extragalactic background light from the multiwavelength *HST*/CANDELS survey in the *Fermi* and CTA era. *Mon. Not. R. Astron. Soc.* **2021**, *507*, 5144.
27. Corianò, C.; Irges, N. Windows over a new low energy axion. *Phys. Lett. B* **2007**, *651*, 298.

28. Corianò, C.; Irges, N.; Morelli, S. Stückelberg axions and the effective action of anomalous abelian models 1. A unitarity analysis of the Higgs-axion mixing. *JHEP* **2007**, *07*, 008.
29. Baer, H.; Krami, S.; Sekmen, S.; et al. Dark matter allowed scenarios for Yukawa-unified SO(10) SUSY GUTs. *JHEP* **2008**, *03*, 056.
30. Baer, H.; Summy, H. SO (10) SUSY GUTs, the gravitino problem, non-thermal leptogenesis and axino dark matter. *Phys. Lett. B* **2008**, *666*, 5.
31. Baer, H.; Haider, M.; Kraml, S.; et al. Cosmological consequences of Yukawa-unified SUSY with mixed axion/axino cold and warm dark matter. *JCAP* **2009**, *02*, 002.
32. Chang, S.; Tazawa, S.; Yamaguchi, M. Axion model in extra dimensions with TeV scale gravity. *Phys. Rev. D* **2000**, *61*, 084005.
33. Dienes, K.R.; Dudas, E.; Gherghetta, T. Invisible axions and large-radius compactifications. *Phys. Rev. D* **2000**, *62*,
34. Jaeckel, J.; Ringwald, A. The Low-Energy Frontier of Particle Physics. *Ann. Rev. Nucl. Part. Sci.* **2010**, *60*, 405–437.
35. Ringwald, A. Exploring the role of axions and other WISPs in the dark universe. *Phys. Dark Univ.* **2012**, *1*, 116–135.
36. Galanti, G.; Roncadelli, M. Axion-like Particles Implications for High-Energy Astrophysics. *Universe* **2022**, *8*, 253.
37. Galanti, G. Axion-like Particle Effects on Photon Polarization in High-Energy Astrophysics. *Universe* **2024**, *10*, 312.
38. Galanti, G. Blazars as Probes for Fundamental Physics. *Universe* **2025**, *11*, 327.
39. Turok, N. Almost-Goldstone Bosons from Extra-Dimensional Gauge Theories. *Phys. Rev. Lett.* **1996**, *76*, 1015.
40. Witten, E. Some properties of O(32) superstrings. *Phys. Lett. B* **1984**, *149*, 351.
41. Conlon, J.P. The QCD axion and moduli stabilisation. *JHEP* **2006**, *2006*, 078.
42. Svrcek, P.; Witten, E. Axions in string theory. *JHEP* **2006**, *2006*, 051.
43. Conlon, J.P. Seeing an Invisible Axion in the Supersymmetric Particle Spectrum. *Phys. Rev. Lett.* **2006**, *97*, 261802.
44. Choi, K.-S.; Kim, I.-W.; Kim, J.E. String compactification, QCD axion and axion–photon–photon coupling. *JHEP* **2007**, *2007*, 116.
45. Arvanitaki, A.; Dimopoulos, S; Dubovsky, S; et al. String axiverse. *Phys. Rev. D* **2010**, *81*, 123530.
46. Acharya, B.S.; Bobkov, K.; Kumar, P. An M theory solution to the strong CP-problem, and constraints on the axiverse. *JHEP* **2010**, *11*, 105.
47. Cicoli, M.; Goodsell, M.; Ringwald, A. The type IIB string axiverse and its low-energy phenomenology. *JHEP* **2012**, *10*, 146.
48. Dias, A.G.; Machado, A.C.B.; Nishi, C.C.; et al. The quest for an intermediate-scale accidental axion and further ALPs. *JHEP* **2014**, *2014*, 037.
49. Cicoli, M. Global D-brane models with stabilised moduli and light axions. *Phys. J. Conf. Ser.* **2014**, *485*, 012064.
50. Conlon, J.C.; Day, F. 3.55 keV photon lines from axion to photon conversion in the Milky Way and M31. *JCAP* **2014**, *11*, 033.
51. Cicoli, M.; Conlon, J.C.; Marsh, M.C.D.; et al. 3.55 keV photon line and its morphology from a 3.55 keV axionlike particle line. *Phys. Rev. D* **2014**, *90*, 023540.
52. Kralijc, D.; Rummel, M.; Conlon, J.C. ALP conversion and the soft X-ray excess in the outskirts of the Coma cluster. *JCAP* **2015**, *2015*, 011.
53. Cicoli, M.; Diaz, V.A.; Guidetti, V.; et al. The 3.5 keV line from stringy axions. *JHEP* **2017**, *10*, 192.
54. Scott, M.J.; Marsh, D.J.E.; Pongkitivanichkul, C.; et al. Spectrum of the axion dark sector. *Phys. Rev. D* **2017**, *96*, 083510.
55. Conlon, J.P. Searches for 3.5 keV absorption features in cluster AGN spectra. *Mon. Not. R. Astron. Soc.* **2018**, *1*, 348–352.
56. Cisterna, A.; Hassaine, M.; Oliva, J.; et al. Axionic black branes in the $k$-essence sector of the Horndeski model. *Phys. Rev. D* **2017**, *96*, 124033.
57. Cisterna, A.; Erices, C.; Kuang, X.-M.; et al. Axionic black branes with conformal coupling. *Phys. Rev. D* **2018**, *97*, 124052.
58. Kim, J.H. Light pseudoscalars, particle physics and cosmology. *Phys. Rep.* **1987**, *150*, 1–177.
59. Cheng, H.Y. The strong CP problem revisited. *Phys. Rep.* **1988**, *158*, 1–89.
60. Kim, J.E.; Carosi, G. Axions and the strong CP problem. *Rev. Mod. Phys.* **2010**, *82*, 557.
61. Maiani, L.; Petronzio, R.; Zavattini, E. Effects of nearly massless, spin-zero particles on light propagation in a magnetic field. *Phys. Let. B* **1986**, *175*, 359.
62. De Angelis, A.; Roncadelli, M.; Mansutti, O. Evidence for a new light spin-zero boson from cosmological gamma-ray propagation? *Phys. Rev. D* **2007**, *76*, 121301.
63. Simet, M.; Hooper, D.; Serpico, P.D. Milky Way as a kiloparsec-scale axionscope. *Phys. Rev. D* **2008**, *77*, 063001.
64. Sánchez-Conde, M.A.; Paneque, D.; Bloom, E.; et al. Hints of the existence of axionlike particles from the gamma-ray spectra of cosmological sources. *Phys. Rev. D* **2009**, *79*, 123511.
65. De Angelis, A.; Galanti, G.; Roncadelli, M. Relevance of axionlike particles for very-high-energy astrophysics. *Phys. Rev. D* **2011**, *84*, 105030; Erratum in *Phys. Rev. D* **2013**, *87*, 109903.
66. Tavecchio, F.; Roncadelli, M.; Galanti, G.; et al. Evidence for an axion-like particle from PKS 1222+216? *Phys. Rev. D* **2012**, *86*, 085036.
67. Wouters, D.; Brun, P. Irregularity in gamma ray source spectra as a signature of axionlike particles. *Phys. Rev. D* **2012**, *86*, 043005.
68. Tavecchio, F.; Roncadelli, M.; Galanti, G. Photons to axion-like particles conversion in Active Galactic Nuclei. *Phys. Lett.*

*B* **2015**, *744*, 375–379.
69. Kohri, K.; Kodama, H. Axion-like particles and recent observations of the cosmic infrared background radiation. *Phys. Rev. D* **2017**, *96*, 051701.
70. Galanti, G.; Tavecchio, F.; Roncadelli, M.; et al. Blazar VHE spectral alterations induced by photon-ALP oscillations. *Mon. Not. R. Astron. Soc.* **2019**, *487*, 123.
71. Galanti, G.; Roncadelli, M.; De Angelis, A.; et al. Hint at an axion-like particle from the redshift dependence of blazar spectra. *Mon. Not. R. Astron. Soc.* **2020**, *493*, 1553.
72. Jain, P.; Panda, S.; Sarala, S. Electromagnetic polarization effects due to axion-photon mixing. *Phys. Rev. D* **2002**, *66*, 085007.
73. Bassan, N.; Mirizzi, A.; Roncadelli, M. Axion-like particle effects on the polarization of cosmic high-energy gamma sources. *JCAP* **2010**, *05*, 010.
74. Agarwal, N.; Kamal, A.; Jain, P. Alignments in quasar polarizations: Pseudoscalar-photon mixing in the presence of correlated magnetic fields. *Phys. Rev. D* **2011**, *83*, 065014.
75. Payez, A.; Cudell, J.R.; Hutsemékers, D. Can axionlike particles explain the alignments of the polarizations of light from quasars? *Phys. Rev. D* **2011**, *84*, 085029.
76. Perna, R.; Ho, W.C.G.; Verde, L.; et al. Signatures of photon-axion conversion in the thermal spectra and polarization of neutron stars. *Astrophys. J.* **2012**, *748*, 116.
77. Day, F.; Krippendorf, S. Searching for axion-like particles with X-ray polarimeters. *Galaxies* **2018**, *6*, 45.
78. Galanti, G. Photon-ALP interaction as a measure of initial photon polarization. *Phys. Rev. D* **2022**, *105*, 083022.
79. Galanti, G. Photon-ALP oscillations inducing modifications to photon polarization. *Phys. Rev. D* **2023**, *107*, 043006.
80. Galanti, G.; Roncadelli, M.; Tavecchio, F.; et al. ALP induced polarization effects on photons from galaxy clusters. *Phys. Rev. D* **2023**, *107*, 103007.
81. Galanti, G.; Roncadelli, M.; Tavecchio, F. ALP-induced polarization effects on photons from blazars. *Phys. Rev. D* **2023**, *108*, 083017.
82. Raffelt, G.G.; Stodolsky, L. Mixing of the photon with low-mass particles. *Phys. Rev. D* **1988**, *37*, 1237.
83. Galanti, G.; Roncadelli, M. Extragalactic photon–axion-like particle oscillations up to 1000 TeV. *JHEAp* **2018**, *20*, 1–17.
84. Dessert, C.; Dunsky, D.; Safdi, B.R. Upper limit on the axion-photon coupling from magnetic white dwarf polarization. *Phys. Rev. D* **2022**, *105*, 103034.
85. Levan, A.J.; Lamb, G.P.; Schneider, B.; et al. The First JWST Spectrum of a GRB Afterglow: No Bright Supernova in Observations of the Brightest GRB of all Time, GRB 221009A. *Astrophys. J. Lett.* **2023**, *946*, L28.
86. Blanchard, P.K.; Villar, V.A.; Chornock, R.; et al. JWST Observations of the Extraordinary GRB 221009A Reveal an Ordinary Supernova Without Signs of r-Process Enrichment in a Low-Metallicity Galaxy. *Nature Astron.* **2024**, *8*, 774.
87. Derishev, E. Relating quasi-stationary one zone emission models to expanding relativistic shocks. *Mon. Not. R. Astron. Soc.* **2023**, *519*, 377.
88. Blanchard, P.K.; Berger, E.; Fong, W. The Offset and Host Light Distributions of Long Gamma-Ray Bursts: A New View from HST Observations of Swift Bursts. *Astrophys. J.* **2016**, *817*, 144.
89. Lyman, J.D.; Levan, A.J.; Tanvir, N.R.; et al. The host galaxies and explosion sites of long-duration gamma-ray bursts: Hubble Space Telescope near-infrared imaging. *Mon. Not. R. Astron. Soc.* **2017**, *467*, 1795–1817.
90. Elmegreen, B.G.; Scalo, J. Interstellar Turbulence I: Observations and Processes. *Annu. Rev. Astron. Astrophys.* **2004**, *42*, 211.
91. Pshirkov, M.S.; Tinyakov, P.G.; Urban, F.R. New Limits on Extragalactic Magnetic Fields from Rotation Measures. *Phys. Rev. Lett.* **2016**, *116*, 191302.
92. Alves Batista, R.; Saveliev, A. The Gamma-Ray Window to Intergalactic Magnetism. *Universe* **2021**, *7*, 223.
93. Neronov, A.; Vovk, I. Evidence for Strong Extragalactic Magnetic Fields from Fermi Observations of TeV Blazars. *Science* **2010**, *328*, 5974.
94. Tavecchio, F.; Ghisellini, G.; Foschini, L.; et al. The intergalactic magnetic field constrained by Fermi/Large Area Telescope observations of the TeV blazar 1ES0229+200. *Mon. Not. R. Astron. Soc.* **2010**, *406*, L70.
95. Tavecchio, F.; Ghisellini, G.; Bonnoli, G.; et al. Extreme TeV blazars and the intergalactic magnetic field. *Mon. Not. R. Astron. Soc.* **2011**, *414*, 3566.
96. Dolag, K.; Kachelriess, M.; Ostapchenko, S.; et al. Lower Limit on the Strength and Filling Factor of Extragalactic Magnetic Fields. *Astrophys. J. Lett.* **2011**, *727*, L4.
97. Dermer, C.D.; Cavadini, M.; Razzaque, S.; et al. Time Delay of Cascade Radiation for TeV Blazars and the Measurement of the Intergalactic Magnetic Field. *Astrophys. J.* **2011**, *733*, L21.
98. Abramowski, A.; Aharonian, F.; Ait Benkhali, F.; et al. Search for extended $\gamma$-ray emission around AGN with H.E.S.S. and Fermi-LAT. *Astron. Astrophys.* **2014**, *562*, 145.
99. Archambault, S.; Archer, A.; Benbow, W.; et al. Search for Magnetically Broadened Cascade Emission from Blazars with VERITAS. *Astrophys. J.* **2017**, *835*, 288.
100. Aharonian, F.; Aschersleben, J.; Backes, M.; et al. [H.E.S.S. Collaboration]. Constraints on the Intergalactic Magnetic Field Using Fermi-LAT and H.E.S.S. Blazar Observations. *Astrophys. J. Lett.* **2023**, *950*, L16.
101. Kronberg, P.P. Extragalactic magnetic fields. *Rept. Prog. Phys.* **1994**, *57*, 325.

102. Grasso, D.; Rubinstein, H.R. Magnetic fields in the early Universe. *Phys. Rep.* **2001**, *348*, 163.
103. Rees, M.J.; Setti, G. Model for the Evolution of Extended Radio Sources. *Nature* **1968**, *219*, 127.
104. Hoyle, F. Magnetic Fields and Highly Condensed Objects. *Nature* **1969**, *223*, 936.
105. Kronberg, P.P.; Lesch, H.; Hopp, U. Magnetization of the Intergalactic Medium by Primeval Galaxies. *Astrophys. J.* **1999**, *511*, 56.
106. Furlanetto, S.; Loeb, A. Intergalactic Magnetic Fields from Quasar Outflows. *Astrophys. J.* **2001**, *556*, 619.
107. Galanti, G.; Roncadelli, M. Behavior of axionlike particles in smoothed out domainlike magnetic fields. *Phys. Rev. D* **2018**, *98*, 043018.
108. Kartavtsev, A.; Raffelt, G.; Vogel, H. Extragalactic photon-ALP conversion at CTA energies. *JCAP* **2017**, *01*, 024.
109. Dobrynina, A.; Kartavtsev, A.; Raffelt, G. Photon-photon dispersion of TeV gamma rays and its role for photon-ALP conversion. *Phys. Rev. D* **2015**, *91*, 083003; Erratum in *IBID* **2015**, *91*, 109902.
110. Jansson, R.; Farrar, G.R. A New Model of the Galactic Magnetic Field. *Astrophys. J.* **2012**, *757*, 14.
111. Jansson, R.; Farrar, G.R. The Galactic Magnetic Field. *Astrophys. J.* **2012**, *761*, L11.
112. Beck, M.C.; Beck, A.M.; Beck, R.; et al. New constraints on modeling the random magnetic field of the MW. *JCAP* **2016**, *05*, 056.
113. Pshirkov, M.S.; Tinyakov, P.G.; Kronberg, P.P.; et al. Deriving the Global Structure of the Galactic Magnetic Field from Faraday Rotation Measures of Extragalactic Sources. *Astrophys. J.* **2011**, *738*, 192.
114. Yao, J.M.; Manchester, R.N.; Wang, N. A New Electron-density Model for Estimation of Pulsar and FRB Distances. *Astrophys. J.* **2017**, *835*, 29.
115. Aghanim, N.; Akrami, Y.; Ashdown, M.; et al. [PLANCK Collaboration]. Planck 2018 results. VI. Cosmological parameters. *Astron. Astrophys.* **2020**, *641*, A6.
116. Aiola, S; Calabrese, E.; Maurin, L.; et al. [ACT Collaboration]. The Atacama Cosmology Telescope: DR4 maps and cosmological parameters. *JCAP* **2020**, *12*, 047.
117. Balkenhol, L.; Dutcher, D.; Ade, P.A.R.; et al. [SPT-3G Collaboration]. Constraints on ΛCDM extensions from the SPT-3G 2018 *EE* and *TE* power spectra. *Phys. Rev. D* **2021**, *104*, 083509.
118. Efstathiou, G.; Gratton, S. The evidence for a spatially flat Universe. *Mon. Not. R. Astron. Soc.* **2020**, *496*, L91.
119. Ross, A.J.; Samushia, L.; Howlett, C.; et al. The clustering of the SDSS DR7 main Galaxy sample—I. A 4 per cent distance measure at $z = 0.15$. *Mon. Not. R. Astron. Soc.* **2015**, *449*, 835.
120. Alam, S.; Ata, M.; Bailey, S.; et al. [BOSS Collaboration]. The clustering of galaxies in the completed SDSS-III Baryon Oscillation Spectroscopic Survey: Cosmological analysis of the DR12 galaxy sample. *Mon. Not. R. Astron. Soc.* **2017**, *470*, 2617.
121. Brieden, S.; Gil-Marín, H.; Verde, L. Model-agnostic interpretation of 10 billion years of cosmic evolution traced by BOSS and eBOSS data. *JCAP* **2022**, *08*, 024.
122. Guth, A.H. Inflationary universe: A possible solution to the horizon and flatness problems. *Phys. Rev. D* **1981**, *23*, 347.
123. Starobinsky, A.A. A new type of isotropic cosmological models without singularity. *Phys. Lett. B* **1980**, *91*, 99.
124. Linde, A. A new inflationary universe scenario: A possible solution of the horizon, flatness, homogeneity, isotropy and primordial monopole problems. *Phys. Lett. B* **1982**, *108*, 389.
125. Amelino-Camelia, G.; Ellis, J.R.; Mavromatos, N.E.; et al. Tests of quantum gravity from observations of $\gamma$-ray bursts. *Nature* **1998**, *393*, 763.
126. Liberati, S.; Maccione, L. Lorentz Violation: Motivation and new constraints. *Ann. Rev. Nucl. Part. Sci.* **2009**, *59*, 245.
127. Ellis, J.; Farakos, K.; Mavromatos, N.E.; et al. Astrophysical Probes of the Constancy of the Velocity of Light. *Astrophys. J.* **2000**, *535*, 139.
128. Amelino-Camelia, G. Quantum-Spacetime Phenomenology. *Living Rev. Rel.* **2013**, *16*, 5.
129. Liberati, S. Tests of Lorentz invariance: A 2013 update. *Class. Quant. Grav.* **2013**, *30*, 133001.
130. Galanti, G.; Tavecchio, F.; Landoni, M. Fundamental physics with blazar spectra: A critical appraisal. *Mon. Not. R. Astron. Soc.* **2020**, *491*, 5268.
131. Addazi, A.; Alvarez-Muniz, J.; Alves Batista, R.; et al. Quantum gravity phenomenology at the dawn of the multi-messenger era—A review. *Progr. in Part. and Nucl. Phys.* **2022**, *125*, 103948.
132. Alves Batista, R.; Amelino-Camelia, G.; Boncioli, D.; et al. White paper and roadmap for quantum gravity phenomenology in the multi-messenger era. *Class. Quant. Grav.* **2025**, *42*, 032001.
133. Gonzales-Mestres, L. Superluminal Particles and High-energy Cosmic Rays. *arXiv* **1997**, arXiv:9706022.
134. Coleman, S.; Glashow, S.L. High-energy tests of Lorentz invariance. *Phy. Rev. D* **1999**, *59*, 116008.
135. Kifune, T. Invariance Violation Extends the Cosmic-Ray Horizon? *Astrophys. J. Lett.* **1999**, *518*, L21.
136. Aloisio, R.; Blasi, P.; Ghia, P.L.; et al. Probing the structure of space-time with cosmic rays. *Phy. Rev. D* **2000**, *62*, 053010.
137. Kifune, T. Detection Method and Observed Data of High-Energy Gamma Rays under the Influence of Quantum Gravity. *Astrophys. J.* **2014**, *787*, 4.
138. Fairbairn, M.; Nilsson, A.; Ellis, J.; et al. The CTA sensitivity to Lorentz-violating effects on the gamma-ray horizon. *JCAP* **2014**, *06*, 005.

139. Tavecchio, F.; Bonnoli, G. On the detectability of Lorentz invariance violation through anomalies in the multi-TeV $\gamma$-ray spectra of blazars. *Astron. Astrophys.* **2016**, *585*, A25.
140. Jacob, U.; Piran, T. Lorentz-violation-induced arrival delays of cosmological particles. *JCAP* **2008**, *01*, 031.
141. Stecker, F.W.; Glashow, S.L. New tests of Lorentz invariance following from observations of the highest energy cosmic $\gamma$-rays. *Astropart. Phys.* **2001**, *16*, 97.
142. Finke, J.D.; Razzaque, S. Possible Evidence for Lorentz Invariance Violation in Gamma-Ray Burst 221009A. *Astrophys. J.* **2023**, *942*, L21.
143. Piran, T.; Ofengeim, D.D. Lorentz invariance violation limits from GRB 221009A. *Phys. Rev. D* **2024**, *109*, L081501.
144. Yang, Y.-M.; Bi, X.-J.; Yin, P.-F. Constraints on Lorentz invariance violation from the LHAASO observation of GRB 221009A. *JCAP* **2024**, *04*, 060.
145. Cao, Z.; Aharonian, F.; Axikegu Bai, Y.X.; et al. [LHAASO Collaboration]. Stringent Tests of Lorentz Invariance Violation from LHAASO Observations of GRB 221009A. *Phys. Rev. Lett.* **2024**, *133*, 071501.
146. Ofengeim, D.D.; Piran, T. The 300 TeV photon from GRB 221009A: A Hint at Non-Linear Lorentz Invariance Violation? *Phys. Rev. D* **2025**, *112*, 083055.
147. Maraschi, L.; Ghisellini, G.; Celotti, A. A Jet Model for the Gamma-Ray—emitting Blazar 3C 279. *Astrophys. J.* **1992**, *397*, L5.
148. Dermer, C.; Schleickeiser, R. Model for the High-Energy Emission from Blazars. *Astrophys. J.* **1993**, *416*, 458.
149. Sikora, M.; Begelman, M.; Rees, M.J. Comptonization of Diffuse Ambient Radiation by a Relativistic Jet: The Source of Gamma Rays from Blazars? *Astrophys. J.* **1994**, *421*, 153.
150. Mannheim, K. The proton blazar. *Astron. Astrophys.* **1993**, *269*, 67.
151. Mannheim, K. TeVgamma-rays from proton blazars. *Space Sci. Rev.* **1996**, *75*, 331.
152. Liu, H.T.; Bai, J.M. Absorption of 10–200 GeV Gamma Rays by Radiation from Broad-Line Regions in Blazars. *Astrophys. J. Phys.* **2006**, *653*, 1089.
153. Tavecchio, F.; Mazin, D. Intrinsic absorption in 3C 279 at GeV-TeV energies and consequences for estimates of the extragalactic background light. *Mon. Not. R. Astron. Soc.* **2009**, *392*, L40.
154. Poutanen, J.; Stern, B. GeV Break in blazars as a result of gamma-ray absorption within the broad-line region. *Astrophys. J.* **2010**, *717*, L118.
155. Albert, J.; Aliu, E.; Anderhub, H.; et al. Very-high-energy gamma rays from a distant quasar: How transparent is the universe? *Science* **2008**, *320*, 1752.
156. Wagner, S.; Behera, B. [H.E.S.S. Collaboration]. Hess Observations Of Quasars. *Bull. Am. Astron. Soc.* **2010**, *41*, 660.
157. Aleksić, J.; Antonelli, L.A.; Antoranz, P.; et al. MAGIC Discovery of Very High Energy Emission from the FSRQ PKS 1222+21. *Astrophys. J.* **2011**, *730*, L8.
158. Tanaka, Y.T.; Thompson, D.J.; D'Ammando, F.; et al. Fermi Large Area Telescope Detection of Bright $\gamma$-Ray Outbursts from the Peculiar Quasar 4C +21.35. *Astrophys. J.* **2011**, *733*, 19.
159. Tavecchio, F.; Becerra-Gonzalez, J.; Ghisellini, G.; et al. On the origin of the $\gamma$-ray emission from the flaring blazar PKS 1222+216. *Astron. Astrophys.* **2011**, *534*, 86.
160. Nalewajko, K.; Begelman, M.C.; Cerutti, B.; et al. Sikora, Energetic constraints on a rapid gamma-ray flare in PKS 1222+216. *Mon. Not. R. Astron. Soc.* **2012**, *425*, 2519.
161. Dermer, C.; Murase, K.; Takami, H. Variable gamma-ray emission induced bu ultra-high-energy neutral beams: Applocation to 4C +21.35. *Astrophys. J.* **2012**, *755*, 147.
162. Franceschini, A.; Rodighiero, G. The extragalactic background light revisited and the cosmic photon-photon opacity. *Astron. Astrophys.* **2017**, *603*, 34.
163. Baktash, A.; Horns, D.; Meyer, M. Interpretation of multi-TeV photons from GRB 221009A. *arXiv* **2022**, arXiv:2210.07172.
164. Carenza, P.; Marsh, M.C.D. On ALP scenarios and GRB 221009A. *arXiv* **2022**, arXiv:2211.02010.
165. Troitsky, S.V. Parameters of Axion-Like Particles Required to Explain High-Energy Photons from GRB 221009A. *JETP Letters* **2022**, *116*, 767.
166. Wang, L.; Ma, B.-Q. Axion-photon conversion of GRB221009A. *Phys. Rev. D* **2023**, *108*, 023002.
167. Zhang, G.; Ma, B.-Q. Axion-Photon Conversion of LHAASO Multi-TeV and PeV Photons *Chinese Phys. Lett.* **2023**, *40*, 011401.
168. Troitsky, S.V. Towards a model of photon-axion conversion in the host galaxy of GRB 221009A. *JCAP* **2024**, *01*, 013.
169. González, M.M.; Rojas, D.A.; Pratts, A.; et al. GRB 221009A: A Light Dark Matter Burst or an Extremely Bright Inverse Compton Component? *Astrophys. J.* **2023**, *944*, 178.
170. Nakagawa, S.; Takahashi, F.; Yamada, M.; et al. Axion dark matter from first-order phase transition, and very high energy photons from GRB 221009A. *Phys. Lett. B* **2023**, *839*, 137824.
171. Avila Rojas, D.; Hernández-Cadena, S.; González, M.M.; et al. GRB 221009A: Spectral Signatures Based on ALPs Candidates *Astrophys. J.* **2024**, *966*, 114.
172. Gao, L.-Q.; Bi, X.-J.; Li, J.; et. al Constraints on Axion-like Particles from the Observation of GRB 221009A by LHAASO. *JCAP* **2024**, *01*, 026.
173. Balaji, S.; Ramirez-Quezada, M.E.; Silk, J.; et al. Light scalar explanation for 18 TeV GRB 221009A. *Phys. Rev. D* **2023**,

*107*, 083038.
174. Batista, R.A. GRB 221009A: A potential source of ultra-high-energy cosmic rays. *arXiv* **2022**, arXiv:2210.12855.
175. Mirabal, N. Secondary GeV-TeV emission from ultra-high-energy cosmic rays accelerated by GRB 221009A. *Mon. Not. R. Astron. Soc.* **2023**, *519*, L85.
176. Das, S.; Razzaque, S. Ultrahigh-energy cosmic-ray signature in GRB 221009A. *Astron. Astrophys.* **2023**, *670*, L12.
177. Smirnov, A.Y.; Trautner, A. GRB 221009A Gamma Rays from the Radiative Decay of Heavy Neutrinos? *Phys. Rev. Lett.* **2023**, *131*, 021002.
178. Barnal, L.; Farzan, Y.; Smirnov, A.Y. Neutrinos from GRB 221009A: Producing ALPs and explaining LHAASO anomalous $\gamma$ event. *JCAP* **2023**, *11*, 098.
179. Meszaros, P.; Rees, M.J. Delayed GEV Emission from Cosmological Gamma-Ray Bursts - Impact of a Relativistic Wind on External Matter. *Mon. Not. R. Astron. Soc.* **1994**, *269*, L41.
180. Sari, R.; Piran, T. Predictions for the very early Afterglow and the Optical Flash. *Astrophys. J.* **1999**, *520*, 641.
181. Dermer, C.D.; Chiang, J.; Mitkam, K.E. Beaming, Baryon Loading, and the Synchrotron Self-Compton Component in Gamma-Ray Bursts. *Astrophys. J.* **2000**, *537*, 785.
182. Zhang, B.; Meszaros, P. High-Energy Spectral Components in Gamma-Ray Burst Afterglows. *Astrophys. J.* **2001**, *559*, 110.
183. Foffato, L.; Tavani, M.; Piano, G. Theoretical modeling of the exceptional GRB 221009A afterglow. *Astrophys. J. Lett.* **2024**, *973*, L44.
184. Wang, X.-Y.; Li, Z.; Meszaros, P. GeV-TeV and X-Ray Flares from Gamma-Ray Bursts. *Astrophys. J.* **2006**, *641*, L89.
185. Murase, K.; Toma, K.; Yamazaki, R.; et al. On the Implications of Late Internal Dissipation for Shallow-decay Afterglow Emission and Associated High-energy Gamma-ray Signals. *Astrophys. J.* **2011**, *732*, 77.
186. Zhang, B.T.; Murase, K.; Yuan, C.; et al. External Inverse-Compton Emission Associated with Extended and Plateau Emission of Short Gamma-Ray Bursts: Application to GRB 160821B. *Astrophys. J. Lett.* **2021**, *908*, L36.
187. Murase, K.; Kunihito, I.; Shigehiro, N.; et al. High-energy cosmic-ray nuclei from high- and low-luminosity gamma-ray bursts and implications for multimessenger astronomy. *Phys. Rev. D* **2008**, *78*, 023005.
188. Waxman, E.; Bahcall J.N. Neutrino Afterglow from Gamma-Ray Bursts: $\sim 10^{18}$ eV. *Astrophys. J.* **2000**, *541*, 707.
189. Zhang, B.T.; Murase, K.; Kimura, S.S.; et al. Low-luminosity gamma-ray bursts as the sources of ultrahigh-energy cosmic ray nuclei. *Phys. Rev. D* **2018**, *97*, 083010.
190. Zhang, B.T.; Murase, K.; Ioka, K.; et al. External Inverse-compton and Proton Synchrotron Emission from the Reverse Shock as the Origin of VHE Gamma Rays from the Hyper-bright GRB 221009A. *Astrophys. J. Lett.* **2023**, *947*, L14.
191. Sari, R.; Piran, T. Hydrodynamic Timescales and Temporal Structure of Gamma-Ray Bursts. *Astrophys. J. Lett.* **1995**, *455*, L143.
192. Essey, W.; Kusenko, A. A new interpretation of the gamma-ray observations of distant active galactic nuclei. *Astropart. Phys.* **2010**, *33*, 81.
193. Essey, W.; Kalashev, O.; Kusenko, A.; et al. Line-of-sight Cosmic-ray Interactions in Forming the Spectra of Distant Blazars in TeV Gamma Rays and High-energy Neutrinos. *Astrophys. J.* **2011**, *731*, 51.
194. Murase, K.; Dermer, C.D.; Takami, H.; et al. Blazars as Ultra-high-energy Cosmic-ray Sources: Implications for TeV Gamma-Ray Observations. *Astrophys. J.* **2012**, *749*, 63.
195. Kalashev, O.; Aharonian, F.; Essey, W.; et al. Possibility of multi-TeV secondary gamma rays from GRB221009A. *Phys. Rev. D* **2025**, *112*, 023022.
196. Michalowski, M.J.; Gentile, G.; Hjorth, J.; et al. Massive stars formed in atomic hydrogen reservoirs: HI observations of gamma-ray burst host galaxies. *Astron. Astrophys.* **2015**, *582*, 78.
197. de Ugarte Postigo, A.; Michalowski, M.; Thoene, C.C.; et al. HI and CO spectroscopy of the unusual host of GRB 171205A: A grand design spiral galaxy with a distorted HI field. *arXiv* **2024**, arXiv:2406.16726.
198. Thöne, C.C.; de Ugarte Postigo, A.; Izzo, L.; et al. The host of GRB 171205A in 3D—A resolved multiwavelength study of a rare grand-design spiral GRB host. *Astron. Astrophys.* **2024**, *690*, 66.
199. Dermer, C.D.; Razzaque, S.; Finke, J.D.; et al. Ultra High Energy Cosmic Rays from Black Hole Jets of Radio Galaxies. *New J. Phys.* **2009**, *11*, 065016.
200. Fletcher, A. The Dynamic Interstellar Medium: A Celebration of the Canadian Galactic Plane Survey. *Astron. Soc. Pac. Conf. Series* **2010**, *438*, 197.
201. Vallée, J.P. Magnetic fields in the galactic Universe, as observed in supershells, galaxies, intergalactic and cosmic realms. *New. Astron. Rev.* **2011**, *55*, 91.
202. Beck, R. Magnetic fields in spiral galaxies. *Astron. Astrophys. Rev.* **2016**, *24*, 4.
203. Kronberg, P.P. *Cosmic Magnetic Fields*; Cambridge University Press: Cambridge, UK, 2016.
204. Heesen, V.; Klocke, T.L.; Brüggen, M.; et al. Nearby galaxies in the LOFAR Two-metre Sky Survey. II. The magnetic field-gas relation. *Astron. Astrophys.* **2023**, *669*, 8.
205. Dermer, C.D.; Atoyan, A. Neutral beam model for the anomalous gamma-ray emission component in GRB 941017. *Astron. Astrophys.* **2004**, *418*, L5.
206. Abbasi, R.; Ackermann, M.; Adams, J.; et al. Limits on Neutrino Emission from GRB 221009A from MeV to PeV Using the IceCube Neutrino Observatory. *Astrophys. J. Lett.* **2023**, *946*, L26.

207. Kruiswijk, K.; Brinson, B.; Procter-Murphy, R.; et al. IceCube search for neutrinos from GRB 221009A. *arXiv* **2023**, arXiv:2307.16354.
208. Zheng, Y.G.; Kang, S.J.; Zhu, K.R.; et al. Expected Signature For the Lorentz Invariance Violation Effects on $\gamma - \gamma$ Absorption. *Phys. Rev. D* **2023**, *107*, 083001.
209. Vardanyan, V.; Takhistov, V.; Ata, M.; et al. Revisiting Tests of Lorentz Invariance with Gamma-ray Bursts: Effects of Intrinsic Lags. *Phys. Rev. D* **2023**, *108*, 123023.
210. Li, H.; Ma, B.-Q. Revisiting Lorentz invariance violation from GRB 221009A. *JCAP* **2023**, *10*, 061.
211. Li, H.; Ma, B.-Q. Lorentz invariance violation induced threshold anomaly versus very-high energy cosmic photon emission from GRB 221009A. *Astropart. Phys.* **2023**, *148*, 102831.
212. Li, H.; Ma, B.-Q. Lorentz invariance violation from GRB221009A. *Mod. Phys. Lett. A* **2024**, *39*, 2350201.
213. Vercellone, S.; Bigongiari, C.; Burtovoi, A.; et al. ASTRI Mini-Array core science at the Observatorio del Teide. *J. High Energy Astrophys.* **2022**, *35*, 1.
214. CTAO. Available online: https://www.cta-observatory.org/ (accessed on 27 August 2025).
215. Egorov, A.E.; Topchiev, N.P.; Galper, A.M.; et al. Dark matter searches by the planned gamma-ray telescope GAMMA-400. *JCAP* **2020**, *11*, 049.
216. HAWC. Available online: https://www.hawc-observatory.org/ (accessed on 27 August 2025).
217. Huang, X.; Lamperstorfer, A.S.; Tsai, Y.L.S.; et al. Perspective of monochromatic gamma-ray line detection with the High Energy cosmic-Radiation Detection (HERD) facility onboard China's space station. *Astropart. Phys.* **2016**, *78*, 35–42.
218. Cao, Z.; della Volpe, D.; Liu, S.; et al. The Large High Altitude Air Shower Observatory (LHAASO) Science Book (2021 Edition). *Chin. Phys. C* **2022**, *46*, 035001–035007.
219. TAIGA-HiSCORE. Available online: https://taiga-experiment.info/taiga-hiscore/ (accessed on 27 August 2025).
220. Bähre, R.; Döbrich, B.; Dreyling-Eschweiler, J.; et al. Any light particle search II—Technical design report. *J. Instrum.* **2013**, *8*, T09001.
221. Armengaud, E.; Attié, D.; Basso, S.; et al. Physics potential of the international axion observatory (IAXO). *JCAP* **2019**, *06*, 047.
222. Capparelli, L.M.; Cavoto, G.; Ferretti, J.; et al. Axion-like particle searches with sub-THz photons. *Phys. Dark Univ.* **2016**, *12*, 37.
223. Kahn, Y.; Safdi, B.R.; Thaler, J. Broadband and resonant approaches to axion dark matter detection. *Phys. Rev. Lett.* **2016**, *117*, 141801.
224. Avignone, F.T., III. Potential for large germanium detector arrays for solar-axion searches utilizing the axio-electric effect for detection. *Phys. Rev. D* **2009**, *79*, 035015.
225. Avignone, F.T., III; Crewick, R.J.; Nussinov, S. Can large scintillators be used for solar-axion searches to test the cosmological axion–photon oscillation proposal? *Phys. Lett. B* **2009**, *681*, 122.
226. Avignone, F. T. III; Crewick, R. J.; Nussinov, S. The experimental challenge of detecting solar axion-like particles to test the cosmological ALP-photon oscillation hypotheses. *Astropart. Phys.* **2011**, *34*, 640.